SULPHUR ISOTOPES IN CANYON DIABLO METEOROID IMPACT PRODUCTS

SULPHUR ISOTOPE FRACTIONATION IN TROILITE OXIDATION, EVAPORATION AND DISSOCIATION, AND THE $^{34}S/^{32}S$ RATIOS IN THE CANYON DIABLO METALLIC SPHEROIDS

by

COLIN ERNEST McEWING, B.Sc., M.Sc.

A Thesis

Submitted to the School of Graduate Studies

in Partial Fulfilment of the Requirements

for the Degree

Doctor of Philosophy

McMaster University

October 1976

DOCTOR OF PHILOSOPHY (1976)
(Physics)

McMASTER UNIVERSITY
Hamilton, Ontario

TITLE: Sulphur Isotope Fractionation in Troilite Oxidation, Evaporation and Dissociation, and the $^{34}S/^{32}S$ Ratios in the Canyon Diablo Metallic Spheroids

AUTHOR: Colin Ernest McEwing, B.Sc. (University of New Brunswick)

M.Sc. (University of New Brunswick)

SUPERVISOR: Professor H. G. Thode

NUMBER OF PAGES: xiv, 130

ABSTRACT

Canyon Diablo metallic spheroids are roughly spherical in form, approximately 1 mm in diameter, consist mainly of nickel and iron and are found in conjunction with Canyon Diablo meteorite fragments in the vicinity of Barringer Meteorite Crater, Arizona.

Conventional chemical techniques and a gas source mass spectrometer, using SF_6 as the analysis gas, were used to measure the sulphur contents and $^{34}S/^{32}S$ ratios in spheroid samples of different sizes. Also, material was removed from various depths within the spheroids by means of ablation using a mixer/mill so that the radial dependence of the sulphur contents and $^{34}S/^{32}S$ ratios could be studied. This was the first time that the $^{34}S/^{32}S$ ratios in the Canyon Diablo metallic spheroids have been measured.

It was found that the spheroids are enriched in ^{34}S compared to the Canyon Diablo meteorite fragments and that the enrichment is greater in the smaller spheroids than in the larger ones. Also, the layers nearest the surface are more enriched than the inner portions.

In order to investigate the possible causes of this enrichment the sulphur isotope effects associated with the oxidation, dissociation and evaporation of the meteoritic

mineral troilite, (FeS), were measured. The troilite samples were heated in a furnace at approximately 1200°C in a dry-air atmosphere for oxidation and in a vacuum for dissociation and evaporation. In the oxidation experiment it was found that the residue has a $\delta^{34}S$ value relative to the starting material of approximately -0.33 ‰ apparently independent of the extent of reaction. Also, dissociation and evaporation occur simultaneously in a two-branch reaction with the $\delta^{34}S$ values of the residues strongly dependent on the extent of reaction in a manner similar to the Rayleigh distillation process. The sulphur isotope effects associated with evaporation and dissociation were found to be (+4.8 ± 0.3) ‰ and (+12.9 ± 0.3) ‰ respectively. Consequently, the $\delta^{34}S$ values (relative to the starting material) of the initial products are respectively about -4.8 ‰ and -12.9 ‰. This is the first time that the sulphur isotope effect associated with the high temperature oxidation of troilite has been measured. It is also the first time that the sulphur isotope effect associated with either the vacuum dissociation or evaporation of troilite has been measured. This latter information has proven useful in the interpretation of the sulphur content and $\delta^{34}S$ data obtained from the analyses of lunar soils. The equations governing the relationships between the $\delta^{34}S$ values of the residue and products in two-branch first-order reactions are presented.

Published hypothetical accounts of the events that led to the Canyon Diablo metallic spheroids having their present chemical composition are reviewed and discussed. The following new explanation is presented that is consistent with the isotope ratio data and the chemical compositional differences between the spheroids and the meteorite fragments. It is suggested that the Canyon Diablo meteoroid included a portion containing greater nickel and cobalt contents than do the fragments presently found at the crater site. This portion was shock-melted by the impact and splash-dispersed to form the spheroids. The ^{34}S enrichment occurred when the spheroids lost sulphur by dissociation/evaporation upon exposure to the near-vacuum of the meteoroid's train.

ACKNOWLEDGEMENTS

The author is sincerely grateful to Dr. H. G. Thode for his patient supervision of this work. Dr. Thode suggested the dissociation/evaporation experiment and skillfully instructed the author on the hydrochloric acid sulphur extraction technique. Dr. Thode also arranged for the author to attend the Fifth Lunar Science Conference and provided other financial support. The author has benefited from discussions with Dr. Thode about various aspects of this work.

The author is greatly indebted to Dr. C. E. Rees who was exceedingly generous in donating large amounts of time and energy in various valuable ways. Dr. Rees derived the extent of reaction – $\delta^{34}S$ equations that were essential to the interpretation of the dissociation/evaporation experiment and suggested the ablation technique be used to investigate the radial dependence of the $\delta^{34}S$ values. Dr. Rees also skillfully and patiently instructed the author on the fluorination and mass spectrometry techniques. The author would have experienced great difficulty in completing this work without the encouragement and unselfish aid provided by Dr. Rees.

Mr. Jan Monster maintained the mass spectrometer in good working order to the great benefit of the author. Also, Mr. Monster patiently instructed the author on a number of chemical techniques and provided valuable suggestions and information during numerous discussions. The author gratefully acknowledges the technical assistance and encouragement provided by Mr. Monster.

The author is grateful to Dr. D. L. Scott who designed and built the vacuum apparatus used in part of this work. Dr. Scott also made a number of helpful suggestions concerning the troilite heating experiments.

Mr. E. M. Beaver designed and constructed the automatic digital readout system for the mass spectrometer and helped in various maintenance tasks. Also, Mr. Beaver provided encouragement at various difficult periods during the course of this work. The author wishes to acknowledge the skillful technical aid provided by Mr. Beaver.

The author is grateful to Professor H. P. Schwarcz for aid in obtaining the spheroid samples and in arranging for the author's use of the mixer facilities of the Geology Department of McMaster University.

Useful suggestions were provided by Professors W. B. Clarke and H. P. Schwarcz during numerous discussions.

The author wishes to thank Dr. I. R. Cameron of the

University of New Brunswick, St. John, New Brunswick, for stimulating his interest in meteorites.

The Canyon Diablo metallic spheroid samples were obtained from Dr. C. B. Moore, Director of the Arizona State University Center for Meteorite Studies, Dr. Y. O. Fortier, Director, Geological Survey of Canada, Ottawa, and Dr. G. I. Huss, Director of the American Meteorite Laboratory, Denver, Colorado.

The author also wishes to express his sincere gratitude to his wife who patiently provided much encouragement during the course of this work and to his parents who made it possible by their generosity for him to attend university as an undergraduate.

TABLE OF CONTENTS

TABLE OF CONTENTS
(continued)

LIST OF TABLES

LIST OF TABLES
(continued)

LIST OF TABLES
(continued)

LIST OF FIGURES

CHAPTER 1

INTRODUCTION

A. Isotope Geochemistry

Isotope geochemistry has as its basis the slight differences in the chemical properties of the isotopes of an element. Differences in the chemical properties of the isotopes of hydrogen, carbon, nitrogen, oxygen and other elements have been established both theoretically and experimentally (Thode, 1970). Measurements of variations in the natural abundances of the isotopes have proved useful in the study of biological and geological problems.

Sulphur isotope geochemistry is particularly interesting because of the variety of the chemical forms of sulphur and their widespread occurrence in such diverse materials as sea water, sedimentary rocks, petroleum, primary igneous rocks, volcanic gases, mineral deposits, lunar samples and meteorites. The four stable isotopes of sulphur with their approximate relative abundances are: ^{32}S (95%); ^{33}S (0.7%); ^{34}S (4.2%); and ^{36}S (0.017%). Variations in the $^{34}S/^{32}S$ ratio are usually measured since ^{34}S and ^{32}S are the two most abundant of the sulphur isotopes.

Isotope fractionation can occur under equilibrium conditions or in unidirectional reactions. As an example of the former consider the equilibration of sulphur dioxide and hydrogen sulphide. The isotopic cases involved are:

$$H_2{}^{32}S \rightleftarrows {}^{32}SO_2$$

and

$$H_2{}^{34}S \rightleftarrows {}^{34}SO_2$$

Equations such as these are usually combined to produce the overall isotope equilibrium equation:

$$H_2{}^{34}S + {}^{32}SO_2 \overset{K}{\rightleftarrows} H_2{}^{32}S + {}^{34}SO_2$$

The isotopic equilibrium constant, K, can differ slightly from unity and the extent of this difference, (K-1), is a measure of the equilibrium isotope effect. In the above case

$$K = \frac{[{}^{34}SO_2]}{[{}^{32}SO_2]} \bigg/ \frac{[H_2{}^{34}S]}{[H_2{}^{32}S]} = 1.008 \text{ at } 500°C \text{ (Thode, 1970)}$$

This means that under equilibrium conditions the ${}^{34}S/{}^{32}S$ ratio of the SO_2 is 1.008 times the ${}^{34}S/{}^{32}S$ ratio of the H_2S. It should be noted that in order for the above isotope equilibrium to be established it is necessary to have water present so that reaction paths for the sulphur isotopes are present.

As an example of isotope fractionation occurring in a unidirectional reaction consider the reduction of sulphate ion to hydrogen sulphide. The isotopic cases may be written as:

$$^{32}SO_4^{=} \xrightarrow{k_1} H_2{}^{32}S$$

and

$$^{34}SO_4^{=} \xrightarrow{k_2} H_2{}^{34}S$$

The ratio of the specific rate constants, k_1/k_2, for the two competing reactions can differ from unity and the extent of this difference, (k_1/k_2-1), is a measure of the kinetic isotope effect. In the example cited $k_1/k_2 = 1.025$ at 25°C (Harrison and Thode, 1957). This means that since the $^{32}SO_4^{=}$ species reacts 2.5% faster than the $^{34}SO_4^{=}$ species the H_2S produced at any instant is enriched in ^{32}S or depleted in ^{34}S by this amount (2.5%) relative to the remaining $SO_4^{=}$.

Isotope effects are usually small and isotope ratio differences are more readily measured than absolute isotope ratios due to cancellation of instrumental fractionation effects so that it is usual to express isotope ratio variations in the "del" (δ) notation as follows:

$$\delta^{34}S(‰) = \left[\frac{(^{34}S/^{32}S)_{sample}}{(^{34}S/^{32}S)_{standard}} - 1 \right] \times 1000.$$

The standard used is sulphur extracted from troilite (FeS) from the iron meteorite Canyon Diablo, since it has been suggested (Macnamara and Thode, 1950) that the $^{34}S/^{32}S$ ratio in iron meteorites is near the primordial value for the Earth. Also, Canyon Diablo meteorite fragments are readily available for interlaboratory standardization.

For mass-dependent processes the *$\delta^{33}S$ and *$\delta^{36}S$ values may be derived from the measured $\delta^{34}S$ values since an approximately linear relationship is predicted (Bigeleisen and Wolfsberg, 1958) between the isotope fractionation and the mass difference between the isotopes involved. For sulphur the relationship $\delta^{34}S \approx 1.94\ \delta^{33}S$ and the relationship $\delta^{36}S \approx 1.90\ \delta^{34}S$ were derived by Hulston (1964). Thus, the $^{34}S/^{32}S$, $^{33}S/^{32}S$ and $^{36}S/^{32}S$ ratios may be used to distinguish a mass-dependent isotope effect, either chemical or physical, from a nuclear effect. By using the above relationships and measurements of the $\delta^{34}S$, $\delta^{33}S$ and $\delta^{36}S$ values Hulston and Thode (1965) found conclusive evidence of cosmic-ray spallation ^{36}S and ^{33}S in the nickel-iron phase of a number of meteorites.

It is shown in Fig. 1 that there is a range of ~130 ‰ in the $\delta^{34}S$ values of terrestrial materials. Discussion of the $\delta^{34}S$ values in all of the materials shown in Fig. 1 has been presented elsewhere (Thode, 1970; Thode, 1963, and

---

*replace ^{34}S with ^{33}S or ^{36}S in the definition of $\delta^{34}S$

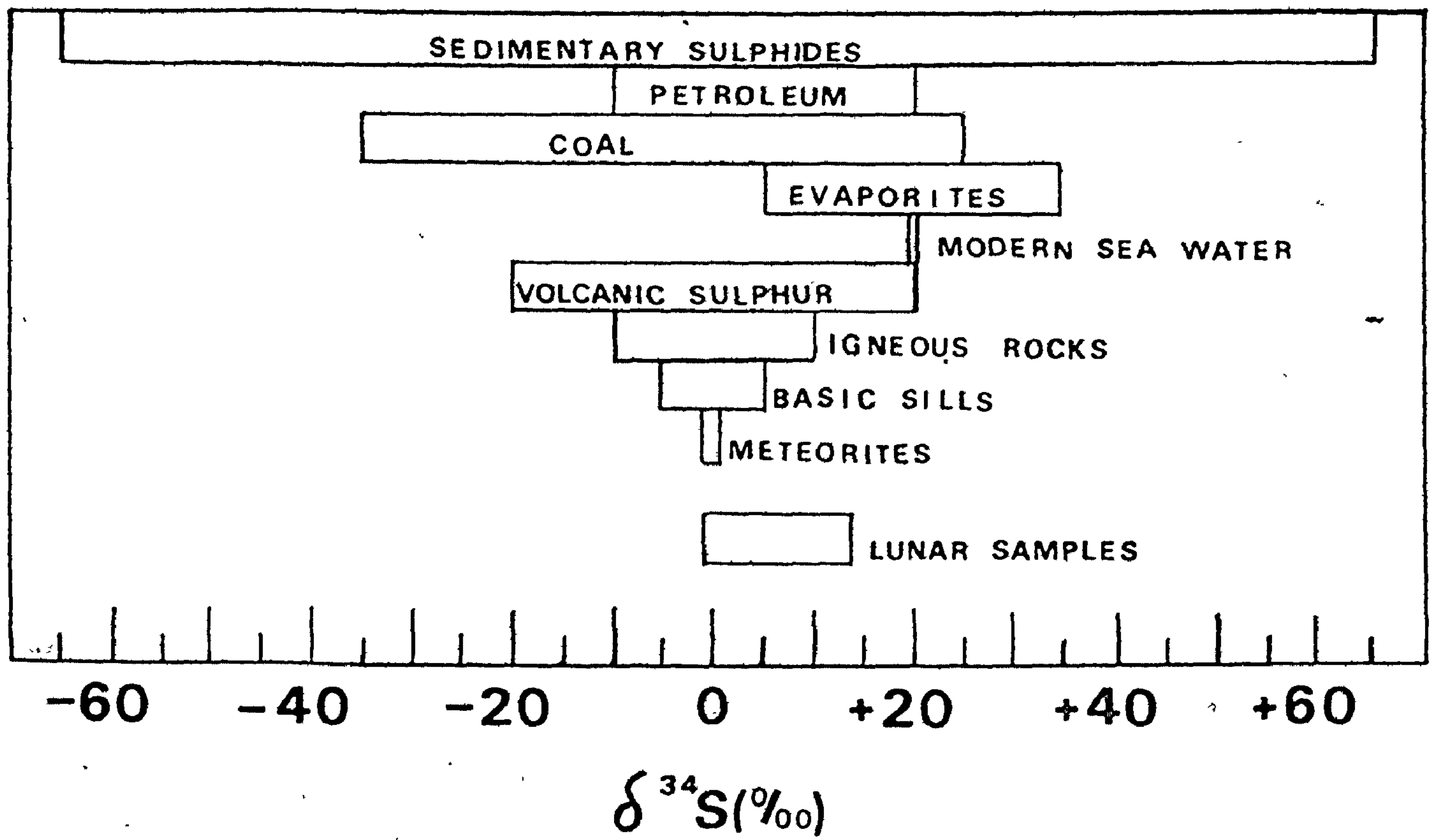

Figure 1. Sulphur isotope distribution in nature (after Thode, 1970)

references therein) so that only a few general comments will be made here. Sulphur which was involved in the sedimentary cycle such as that in coal and petroleum displays a wide range of $\delta^{34}S$ values. This range is believed largely due to the metabolic activity of bacteria (Desulfovibrio desulfuriccans) which reduce sulphate to hydrogen sulphide in anaerobic environments. Previously it was stated that the kinetic isotope effect in the chemical reduction of sulphate was 2.5% or 25‰. However, the bacterial reduction of sulphate is a complex process (Rees, 1973) and in nature a 0‰ to 50‰ kinetic isotope effect is observed depending on the environmental conditions.

Sulphur in basic sills and igneous rocks of primary origin has not been involved in the sedimentary cycle and so it displays a narrower range of $\delta^{34}S$ values close to zero. Some of this range is believed to be due to the small equilibrium isotope effects between coexisting sulphide minerals. For example, at chemical equilibrium, the differences between the $\delta^{34}S$ values of coexisting galena (PbS) and sphalerite (ZnS) are of the order of 2‰ (Lusk and Crocket, 1969) depending on the temperature of equilibrium.

The principal form of sulphur in meteorites is troilite (FeS) although small amounts of other sulphur compounds such as daubreelite ($FeCr_2S_4$), oldhamite (CaS), and pentlandite [$(Fe,Ni)_9S_8$] have been found in some meteorites. The range of $\delta^{34}S$ values in meteorites is very small compared to the overall range in terrestrial samples. Thode, Monster and Dunford (1961) measured the $\delta^{34}S$ values in seventeen meteorites of various classifications and found a range from -0.3‰ to +0.2‰ (measured from the mean value).

A relatively rare class of meteorites, the carbonaceous chondrites, contain some sulphur in different oxidation states so that a larger range of $\delta^{34}S$ values than in other meteorite classes might be expected. Monster, Anders and Thode (1965) measured the $\delta^{34}S$ values in Orgueil, a carbonaceous chondrite, and found a value of -1.5‰ for the sulphate sulphur and +3.0‰ for the elemental sulphur although the weighted average for the two forms of sulphur was close to 0.0‰.

The sulphur contents and $\delta^{34}S$ values of lunar samples from all the Apollo flights have been measured. Thode and Rees (1976) found the $\delta^{34}S$ values for the lunar basaltic rocks to lie between $\sim$0.2‰ and 0.7‰, while Gibson et al. (1975) and Petrouski, Kerridge and Kaplan (1974) found values ranging from -1.6‰ to +2.0‰ respectively. The $\delta^{34}S$ values for the lunar "soils" lie between roughly -3‰ (Chang, Lennon and Gibson, 1974) and +13‰ (Kerridge, Kaplan and Petrouski, 1975). For a discussion of these results and the distribution of $\delta^{34}S$ values and sulphur concentrations throughout the lunar soils of different grain size see Rees and Thode (1974), and Thode and Rees (1976).

B. The Canyon Diablo Metallic Spheroids

The asteroids, which are found mainly in the asteroid belt between Mars and Jupiter, are surviving fragments from collisions between relatively small planetary bodies (Chapman, 1975). The usual orbit of an asteroid may be perturbed by collision or gravitation so that it may eventually enter the Earth's atmosphere where part of its kinetic energy is transformed into heat and light. The resultant streak of light observed in the sky is called a meteor and the body producing the streak of light is called a meteoroid. The heating of the meteoroid's surface causes portions of it to melt and be swept away so that a fraction of the meteoroid's initial mass is lost by this atmospheric ablation. It is also common for the meteoroid to break apart during its passage through the atmosphere. Once the meteoroid makes contact with the ground it is called a meteorite.

The smaller meteoroids are decelerated more by the atmosphere than are the larger ones. Meteoroids with initial masses up to a ton lose virtually all their preatmospheric velocity before striking the ground but those with initial masses of ten tons or more retain considerable fractions of their preatmospheric velocities. For instance, if vertical infall and an initial speed of 40 km/sec are assumed then a meteoroid of 1,000 tons initial mass or greater retains more than a half of its preatmospheric geocentric velocity (Mason, 1962).

Thousands of geocentric meteor velocities have been measured at the earliest section of their trail (Bjork, 1961) and they all have been found to be within the range from $\sim$11 km/sec (the escape velocity from Earth) to $\sim$72 km/sec (the maximum geocentric velocity for a body belonging to the solar system). The average geocentric meteor velocity has been found to be $\sim$15 km/sec (Kinslow, 1965).

Exactly what occurs when a massive meteoroid collides with the Earth at meteoric velocities is not perfectly understood [see (Chao, 1974) and (Charters, 1960)]. Velocities of only $\sim$10 km/sec have been attained in the laboratory and it is difficult to scale the small pellet impacts to impacts with meteoroids weighing thousands of tons. The kinetic energy per unit mass of bodies travelling at meteoric velocities is of the same order as the explosive energy per unit mass of TNT ($\sim 10^{11}\ \frac{\text{ergs}}{\text{gm}}$) and shock pressures of 10 million atmospheres, about three times the pressure at the center of the Earth, or greater, may be attained upon impact (Bjork, 1961). Since shock pressures of 2 Mb (1 Mb $\sim 10^6$ atmospheres) are sufficient to completely melt iron (Olshaker and Bjork, 1961) it is believed that impacts of this magnitude could vaporize most of the meteoroid and some of the target rock and soil. The explosive expansion of this vapour and the effects of the shock wave combine to form an impact explosion crater. The surfaces of the Moon, Mars, Mercury and Venus have been scarred by the impact explosion craters formed by meteoroids. On the Earth there are about 60 geological structures that are thought to be impact craters (Dence, 1971). Glaciation and other geological processes on the Earth have, of course, erased most of the evidence of older craters.

The most-studied of Earth's meteorite craters is the $\sim$1,200 m diameter Barringer Meteorite Crater in Arizona, U.S.A. The crater is associated with fragments of what is called the Canyon Diablo meteorite. About 20 to 30 tons of the Canyon Diablo meteorite fragments have been collected from the environs of the crater. These fragments are of the octahedrite class of the iron meteorite group. Octahedrites consist primarily of the nickel-iron alloys kamacite and taenite with minor inclusions of schreibersite [$(Fe,Ni)_3P$], troilite (FeS) and cohenite (Fe_3C).

In 1948 H. H. Nininger (1956) separated metallic particles from the soil surrounding the Barringer Meteorite Crater. These particles vary in shape from irregular to elongate to spherical (Mead, Littler and Chao, 1965) and range in size from microscopic to 3-4 mm in diameter (Kelly, Holdsworth and Moore, 1974). The particles consist primarily of metallic nickel-iron with small amounts of cobalt, phosphorus and sulphur (Blau, Axon and Goldstein, 1973) but have a different chemical composition from the Canyon Diablo meteorite fragments. Nininger termed these particles "metallic spheroids" and suggested that they were condensation droplets from the metallic vapour cloud formed by the impact explosion.

J. S. Rinehart (1958) studied the distribution of the metallic spheroids in a 80 square mile area surrounding the crater. He estimated that there was ~12,000 tons of the spheroids in the soil surrounding the crater. The pattern of distribution suggested that the meteoroid approached from a southwesterly direction and pitched forward the liquid spheroids with other non-liquified fragments when it collided with the earth.

Metallic spheroids of the type found at the

Barringer Meteorite Crater are also found elsewhere in nature. Spencer (1933) described similar metallic spheroids in the impactite glass (silica glass bombs) found near the Wabar (Saudi Arabia) and the Henbury (Australia) meteorite craters. Mead, Littler and Chao (1965), and Chao, Dwornik and Littler (1964) have also described metallic spheroids in the impactite glass from the Barringer Meteorite Crater and in southeast Asian tektites. (Tektites are silica glass structures, usually about thumb-size, of debated origin (Mason, 1962) found on the Earth's surface in limited regions on terrains to which they have no apparent genetic associations.) Metallic spheroids have also been found in the lunar material (Goldstein and Yakowitz, 1971) and since meteoroid impacts take place on Mars, Mercury and Venus (Hartmann, 1975) it might be expected that they will also be found on those planets.

There are four different theories in the literature concerning the formation of the Canyon Diablo metallic spheroids. H. H. Nininger (1956) argues that the spheroids condensed from the center of a explosion-produced metallic vapour cloud so that they were not exposed to the atmosphere until after they had condensed and solidified. Low temperature oxidation then destroyed all of the spheroids having compositions different than the ones found today.

Rinehart (1958) suggests that the spheroids were splashed out of the impact-melted meteoroid and were not condensation droplets from a metallic vapour cloud. However, he, like Nininger, suggests that only the spheroids with certain compositions survived the oxidation of weathering.

Blau, Axon and Goldstein (1973) and Kelly, Holdsworth and Moore (1974) also both suggest that the material in the spheroids was never in the vapour phase but was splashed out of a homogeneous liquid formed by the impact event. They also both suggest that the spheroids were oxidized as they flew through the air to land in their present positions. However, Blau et al. maintain that the spheroids were produced from a liquid which was formed only from the sulphide-rich regions of the meteoroid, while Kelly et al. believe that the liquid consisted of a melt formed equally from all regions of the meteoroid.

F. G. Hawley (Nininger, 1956, p. 88) found a sulphur content of 0.96 weight percent in the Canyon Diablo metallic spheroids. There is uncertainty concerning the amount of sulphur in the pre-impact meteoroid since the sulphur is irregularly distributed as nodules of troilite (FeS) in the nickel-iron matrix. Blau et al. believe the spheroids are enriched in sulphur compared to the original meteorite, while Kelly et al. believe the spheroids have lost sulphur. They both suggest that the spheroids have lost some sulphur by oxidation during their flight through the atmosphere after the impact. Since there was a possibility of loss and thus a possibility of isotope fractionation it was decided that a study of the sulphur content and $\delta^{34}S$ values might provide useful information.

In later chapters the experiments that were performed are fully described but a brief summary is provided here. The sulphur content and $\delta^{34}S$ values were first measured to determine if there were any differences in these quantities between the spheroids and the unaltered meteorite fragments. After a $\delta^{34}S$ difference was established then sulphur content and $\delta^{34}S$ measurements were performed on the outer and inner portions of the spheroids to see how these quantities varied with depth.

Since two of the formation theories suggested that the spheroids had been molten, an experiment was carried out to measure the sulphur isotope fractionation, if any, which occurred during the oxidation of troilite (FeS), the only sulphur-bearing mineral in the spheroids (Mead, Littler and Chao, 1965).

Since one of the formation theories suggested that the spheroids condensed out of an oxygen-free atmosphere an experiment was carried out to determine if any sulphur isotope fractionation occurs during the vacuum dissociation of troilite which takes place at $\sim$1200°C.

CHAPTER 2

EXPERIMENTAL

A. Troilite Heating

1. Furnace Description

A Fisher Scientific Company "microcombustion" furnace, which incorporates a specially wound, one-piece Nichrome wire heating coil, was used to heat troilite samples. It could be heated to its maximum temperature, ∿1300°C, in about ten minutes. A thermocouple located between the heating wires in the top of the heating element was used to estimate the temperature of the sample. Diagrams of the furnace and connected apparatus are shown in Fig. 2 and Fig. 3.

2. Troilite Dissociation

The dissociation of troilite experiments were carried out in the following manner. A troilite sample was weighed and placed in a quartz glass tube, sealed at one end and open to the vacuum system at the other (see Fig. 2). The tube was enclosed in a quartz glass sleeve (A in the Figure) to prevent direct contact with the heating wires. The sample was heated under vacuum overnight at a temperature of 400°C to remove any water which could conceivably be

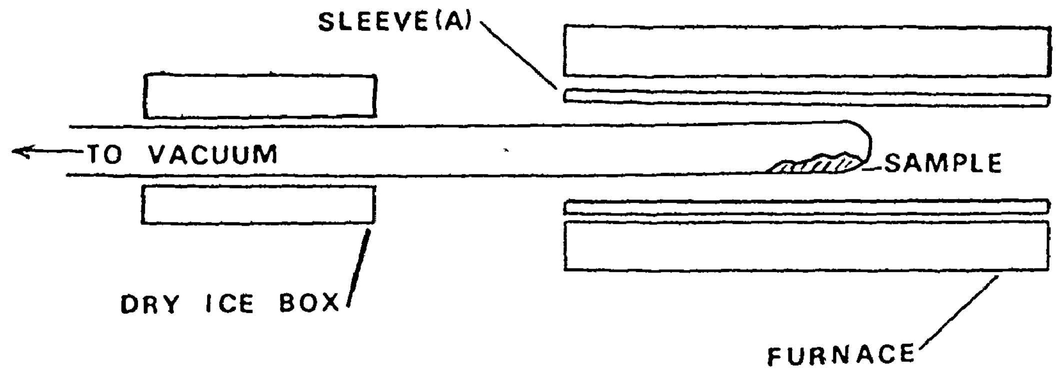

Figure 2. Schematic Diagram of the Dissociation/Evaporation Apparatus

adsorbed on the sample. The temperature was then raised until a value of 1100°C was indicated on the thermocouple gauge. Since this temperature was sufficient to melt the troilite samples the actual temperature of the sample must have been about 1200°C, since troilite melts at $\sim$1196°C (Weast, 1968). A section of the sample tube between the furnace and the vacuum system was surrounded by dry ice to ensure trapping the emitted vapours in a narrow length of tube. The elemental sulphur produced by the dissociation of troilite, and the evaporated troilite condensed on this cold section of the tube. After the duration of the experiment and the cooling of the apparatus the residue section of the tube was separated from the condensed products section. The section containing the residue was placed in a desiccator until later conversion to silver sulphide (see Chapter 3, section 6) while the condensed products section was immediately placed in a Soxhlet apparatus (see Chapter 3, section 5) for the conversion of the elemental sulphur to copper sulphide.

3. Troilite Oxidation

The oxidation of troilite experiments were carried out in the following manner. The troilite was weighed and placed in a quartz capsule closed at one end (see Fig. 3). The capsule was then sealed inside the furnace chamber by

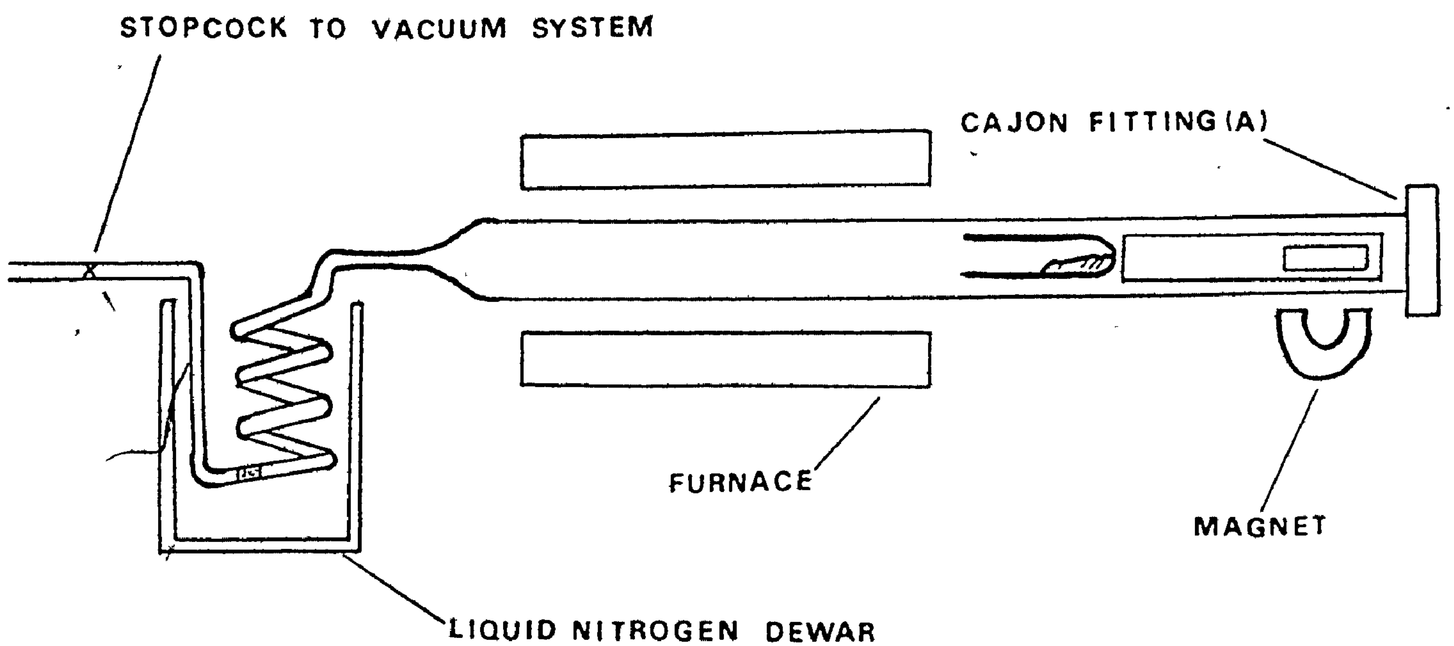

Figure 3. Schematic Diagram of the Oxidation Apparatus

means of a Cajon fitting (A in the figure). The furnace chamber was then evacuated and finally filled with air dried by passing it through a 10 cm column of $CaSO_4$. The capsule was pushed into the center of the furnace by means of the magnetic plunger after the temperature of the furnace was indicated to be 1100°C (see Section 2, above). The sample in the capsule was heated for a predetermined period of time and then removed to the cool regions of the tube. The gas in the chamber was slowly pumped out through a glass coil immersed in liquid nitrogen so that the sulphur dioxide (and possibly some sulphur trioxide) were condensed. The glass coil contained a sintered glass disc near the vacuum end to ensure that none of the solid SO_2 escaped during pumping. The volume of the sulphur dioxide was measured manometrically and it was then transferred to a sample tube where it was stored until ready for further chemical treatment and mass spectrometric analysis.

B. Chemical Conversion Techniques

1. <u>Conversion of SO_2 to $BaSO_4$</u>

The fragile glass tip of the sample tube containing the sulphur dioxide is broken beneath the surface of approximately 400 ml of distilled water contained in a beaker so that the water rises in the tube as the sulphur dioxide dissolves in it. Five ml of saturated bromine water and 1 ml concentrated hydrochloric acid is then added and the solution brought to a boil. Ten ml of a boiling barium chloride solution (10% by weight) is then added and the solution maintained at a boil until the turbidity disappears (usually 45 min.).

The cooled solution is then filtered through Whatman #40 ashless filter paper. The $BaSO_4$ precipitate, after being washed five times with distilled water, is transferred, together with the filter paper, into a crucible and ashed. The remaining $BaSO_4$ is then converted into Ag_2S (see Chapter 3, section 6).

2. Elemental Sulphur Extraction

Elemental sulphur is extracted by means of a Soxhlet extractor using acetone and a piece of copper mesh. The acetone is allowed to boil for about 10 hours during which time the elemental sulphur reacts with the copper mesh to form copper sulphide. The copper mesh is then treated with HCl in a reflux apparatus to form Ag_2S as described below in Section 6.

3. Preparation of Ag_2S

Both sulphides and sulphates are converted to Ag_2S before fluorination. In the case of sulphate sulphur this is done as follows. $BaSO_4$ is boiled with a reducing mixture originally described by Luke (1943) consisting of HCl, HI, and H_3PO_2. The H_2S generated is first precipitated as CdS in a cadmium acetate solution and finally as Ag_2S with the addition of $AgNO_3$ solution. In the case of acid soluble sulphides, H_2S is generated by boiling weighed samples with 8N HCl and the H_2S is precipitated as Ag_2S as described above. The Ag_2S precipitate is washed with NH_4OH to remove any AgCl present and with distilled water four to five times to remove all ion contaminants. This is done by repeating the process of centrifuging, decanting and adding distilled water. The purified Ag_2S is dried, weighed and stored in the aluminium foil weighing packets until subsequent fluorination.

Preliminary experiments showed that 100% of the H_2S generated was recovered as CdS using a single cadmium acetate collector. Standard silica-troilite mixtures were prepared to test the yields obtained by the above procedures.

Table 1 shows that a mean yield of 92.20% was obtained. The standard deviation for an individual measurement was calculated to be $\pm 4.36\%$. These results are for samples yielding about 1.24 mg of sulphur as sulphide.

Additional measurements of the yield and reproducibility were carried out on artificial troilite obtained

TABLE 1

YIELD AND REPRODUCIBILITY MEASUREMENTS

ON ARTIFICIAL TROILITE-SILICA MIXTURE

Sample number	Sample weight (grams)	Silver sulphide weight (milligrams)	Sulphur content (ppm)	*Yield %
1	0.68232	6.97	1,322	95.94
2	0.62774	6.12	1,261	91.51
3	0.62884	6.00	1,235	89.62
4	0.62864	6.30	1,297	94.12
5	0.62792	5.93	1,222	88.68
6	0.62822	6.35	1,308	94.92
7	0.62838	6.00	1,235	89.62
8	0.62845	6.20	1,277	92.67
9	0.62848	6.08	1,252	90.86
10	1.25705	12.91	1,329	96.44
11	1.88502	19.26	1,322	95.94
12	3.13607	33.02	1,362	98.83
13	1.22083	12.05	1,277	92.67
14	0.85848	8.72	1,314	95.36
15	0.84975	8.46	1,288	93.47
16	0.84597	9.01	1,378	100.00
17	0.83645	8.09	1,251	90.78
18	0.83561	8.11	1,256	91.15
19	0.84962	8.32	1,267	91.94
20	0.84911	7.83	1,193	86.57
21	0.85042	8.12	1,235	89.62
22	0.84932	7.89	1,202	87.23
23	0.85076	7.49	1,139	82.66

Mean yield and standard deviation of the mean = $(92.20 \pm 0.84)\%$. Standard deviation of the mean as a % of the mean = $\pm \frac{0.84}{92.20} \times 100\% = \pm 0.91\%$.

Square root of the number of samples multiplied by the standard deviation of the mean as a % of the mean = $\sqrt{23} \times \pm 0.91\% = \pm 4.36\%$.

*Based on the assumption that sample No. 16 was a 100% yield sample.

TABLE 2

YIELD AND REPRODUCIBILITY MEASUREMENTS

ON ARTIFICIAL TROILITE

Sample number	Sample weight (milligrams)	Silver sulphide weight (milligrams)	Weight % S	*Yield %
5.20	7.94	19.82	32.30	89.85
5.21	8.07	20.35	32.63	90.76
5.22	7.52	19.04	32.76	91.13
5.23	6.27	15.27	31.51	87.65
5.24	11.21	27.80	32.09	89.26
5.25	10.00	25.34	32.79	91.21
5.26	10.66	26.98	32.75	91.10
V14	115.46	300.35	33.66	93.63
V15	114.53	297.38	33.60	93.46

Mean yield and standard deviation of the mean = (90.89 ± 0.63)%.

Standard deviation of the mean as a percent of the mean = $\frac{0.63}{90.89} \times 100\% = 0.69\%$.

Square root of the number of samples multiplied by the standard deviation of the mean as a percent of the mean = 2.07%.

*Based on a sulphur content of 35.95% sulphur (see text, page 25 and page 27).

from Cerac/Pure Inc. of Butler, Wisconsin. That company provided a weight percent sulphur content value of 35.95% for that troilite sample from spectrographic analysis (see Chapter 4, section A for more details concerning the handling of this material). The results of the yield and reproducibility measurements are shown in Table 2. A mean yield of 90.89% was obtained which is not significantly different from that obtained using the silica-troilite mixture. The standard deviation of an individual measurement is 2.07%, which is smaller than that obtained using the silica-troilite mixture. Perhaps this is due to a greater water-adsorptive capacity of the fine silica powder.

The major losses are believed to occur because complete removal of silver sulphide from the narrow cadmium acetate solution inlet tube and the centrifuge tube is difficult. These losses are mechanical so that there would be no associated isotope fractionation.

4. Preparation of SF_6

The fluorination of Ag_2S samples to form SF_6 is carried out in the apparatus illustrated in Fig. 4 previously described by Thode and Rees (1974). The apparatus is essentially a vacuum line with a bromine pentafluoride dispensing system (A in the Figure) and nickel

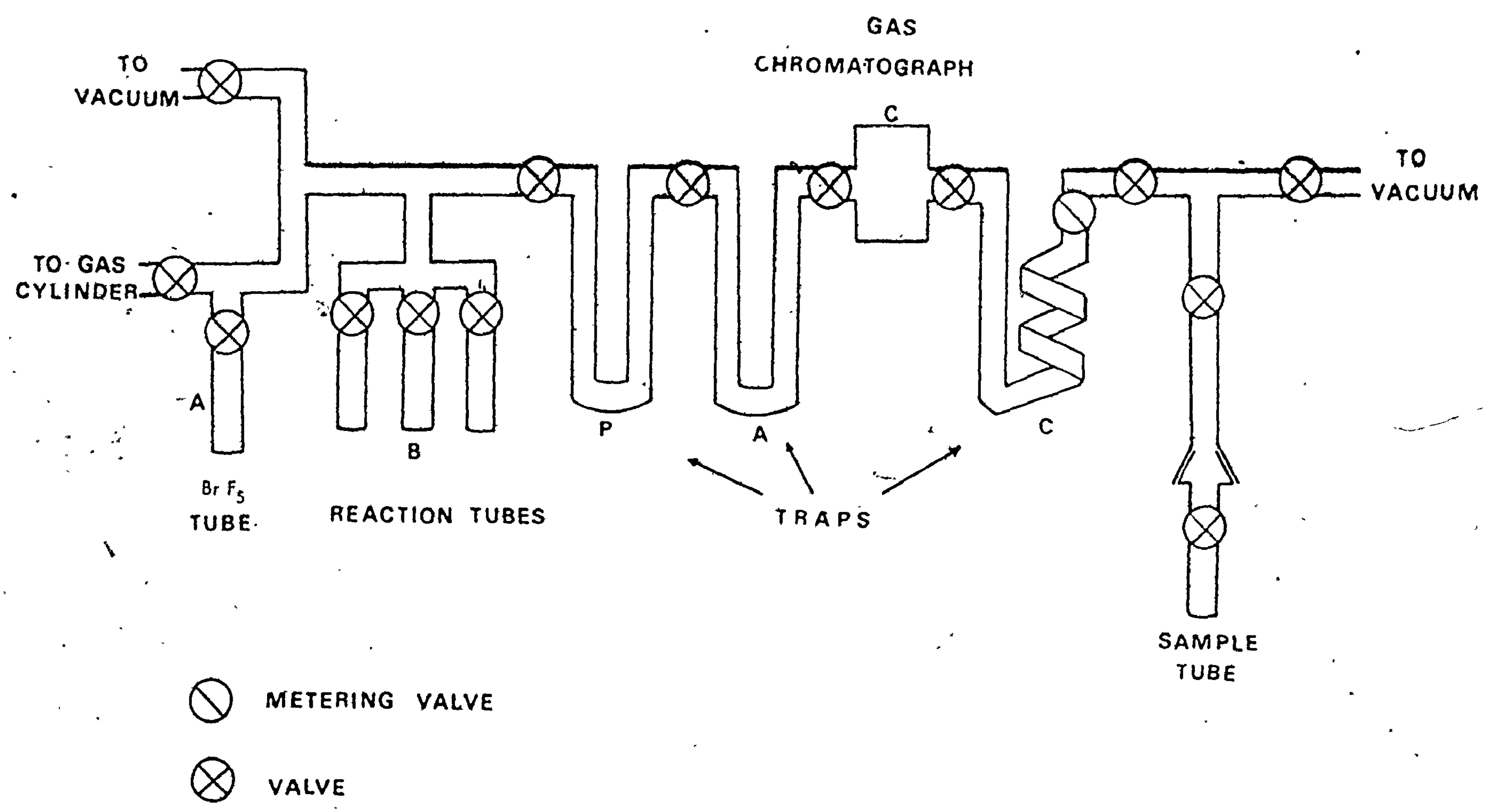

Figure 4. Schematic Diagram of the Fluorination Line

tubes (B) in which the Ag_2S samples are reacted with the BrF_5. A gas chromatograph (C) separates gaseous contaminants from the SF_6. The BrF_5 dispensing system and manifold of reaction tubes is essentially the same as that described by Clayton and Mayeda (1963). The gas chromatograph uses helium as a carrier gas and a coiled six foot column of 1/4" O.D. copper tubing packed with a 5A° molecular sieve. The column is in a furnace so that it may be baked at the end of an operating day but separations are performed at room temperature. The helium flow has its own pathway, separate from the vacuum system of the fluorination line, but there is one bypass route through the input arm of the gas chromatograph (trap A) and another bypass route through the collecting trap (trap C) at the other end of the column.

The silver sulphide sample is wrapped in the aluminium foil boat used in weighing and placed in a reaction tube. The air is then pumped out after which ∿20 x molar excess of BrF_5 is added to the reaction tube. The temperature of the removable furnace placed to enclose the reaction tubes is raised to ∿330°C and this temperature is maintained for about 16 hours. The furnace is then removed and the resultant SF_6 is separated from the unreacted BrF_5 and other reaction products by a combination of vacuum distillations and gas chromatography. After liquid nitrogen baths have been placed on both the reaction tube and trap P, the reaction tube valve is slowly opened and the non-condensables are pumped to waste. A dry ice/acetone bath is then placed on the reaction tube and a five-minute vacuum distillation takes place which transfers virtually all of the SF_6 to trap P. Since a small portion of the SF_6 is occluded by the condensables, the reaction tube valve is then closed and the reaction tube warmed to room temperature to facilitate their release. Then a second vacuum distillation is performed from the reaction tube at dry ice temperature to trap P at liquid nitrogen temperature. A further similar singular vacuum distillation from trap C to the input arm of the gas chromatograph (trap A) is then performed.

After the trap A valve is closed the trap is warmed to room temperature and the helium flow is diverted through the trap so that the SF_6 and unwanted gases are carried through the gas chromatograph column. When a thermal conductivity detector located immediately before the collection trap indicates the passage of SF_6 helium flow is diverted through the second successive diversionary route into the coiled trap, held at liquid nitrogen temperature. After all the SF_6 gas is trapped the helium flow is then diverted to waste so that the unwanted gases are removed from the fluorination line. With trap C held at liquid nitrogen temperature the helium is then all slowly pumped to waste through a metering valve. The trap, with its valve closed, is then warmed to room temperature and the SF_6 is transferred to a valved tube for transportation to the mass spectrometer.

Tests for loss of SF_6 during vacuum handling, for the possible incomplete conversion of sulphur to SF_6 and for memory effects were perfomed (Thode and Rees, 1971) as follows.

1. The residual material from each vacuum distillation during an extraction was itself transferred back to the reaction tube. After gas chromatography of the main SF_6 sample a complete second extraction was performed.

2. After extraction of SF_6 and disposal of residual gases, a fresh dose of BrF_5 was admitted to the reaction tube and a second fluorination and extraction performed.

3. After fluorination and SF_6 extraction the aluminium foil was removed from the reaction tube and an empty piece put in its place. After pump-out and admission of BrF_5 a complete fluorination and extraction were performed.

The amount of SF_6 recovered in each of these three tests was monitored on the thermal conductivity detector and in each case was ≤0.1% of the original amounts involved indicating practically quantitative yields in fluorination and extraction as well as negligible blank levels.

C. Mass Spectrometry

1. The Mass Spectrometer

The following description is essentially the same as that given by Thode and Rees (1971). The 6" radius mass spectrometer and wide slit-narrow slit double collection configuration have been described by Wanless and Thode (1953) and Hulston (1964) respectively. Beaver (1973) has described a number of modifications to the electronics.

The wide slit (low mass) and narrow slit (high mass) Faraday cups are connected to Model 401 Cary vibrating reed electrometers (V.R.E.'s) with input resistors of $5 \times 10^{8}\Omega$ and $10^{10}\Omega$ respectively. The one volt full-scale outputs of each V.R.E. are fed to Hewlett-Packard Model 2212A voltage to frequency convertors (V.F.C.'s) which have outputs of 100 KH/v. The V.F.C. outputs are fed into a Hewlett-Packard Model 5216A counter operating in the ratio mode so that it counts the number of pulses from the narrow slit V.F.C. in the time it takes to accumulate 10^{6} pulses from the wide slit V.F.C. The normal operating $^{32}SF_5^{+}$ ion current is 3×10^{-10} a which gives rise to a 0.5 V signal from the wide slit V.R.E. and a 50 KH signal from its V.F.C. so that the counting period for 10^6 cycles is twenty seconds. At the end of a counting period the counter directly displays the ratio of the ion currents arriving at the narrow and wide slits. Another counting period is then carried out automatically after which the print-out of the ion current ratio activates logic circuitry controlling the magnetic valve sample inlet system (Beaver, 1973) and causes changeover from unknown gas to standard gas or vice versa. A 30-second delay is allowed to facilitate flushing of the previous gas. Cycling continues automatically until five double measurements have been made with the unknown gas and four with the standard. Peak centering is checked by manually switching the accelerating voltage to bring the edge of the $^{34}SF_5^+$ peak to the narrow slit and after recentering the peak of interest another set of measurements is taken. The results of these two sets of measurements are then averaged.

2. Reproducibility of Fluorination and Mass Spectrometry

All samples are run against a mass spectrometer line standard of cylinder SF_6, which is admitted to the spectrometer sample line in 0.7 cm^3 STP aliquots from a reservoir containing 1200 cm^3 STP.

Each day a sample of the same batch of Ag_2S is fluorinated and analysed in the mass spectrometer to measure the reproducibility of the method. If it is also desired to compare the $^{34}S/^{32}S$ ratios of the samples to be analysed to that of the sulphur in Canyon Diablo troilite then a single batch of Ag_2S prepared from Canyon Diablo troilite is used. Alternatively a secondary standard consisting of a single batch of Ag_2S, whose $^{34}S/^{32}S$ ratio relative to Canyon Diablo troilite is well known, is used. The standard deviation of an individual measurement is obtained by multiplying the square root of the number of such analyses by the standard deviation of their mean. The reproducibility for fluorination, plus gas chromatography, plus mass spectrometry indicated by such measurements are usually superior to that obtained in this laboratory by using SO_2 as the analysis gas. The standard deviation of an individual measurement using SO_2 is usually about $\pm 0.2‰$ (Mr. J. Monster, private communication) whereas that obtained by the author using SF_6 has ranged from $\pm 0.03‰$ for one set of standard samples to $\pm 0.18‰$ for another set.

CHAPTER 3

WHOLE SPHEROID AND ABLATED SPHEROID MEASUREMENTS

A. Sample Description

Three different sets of metallic spheroids were analysed during the course of this work. One set was obtained from Dr. Y. O. Fortier, Director of the Geological Survey of Canada, Ottawa, who earlier had obtained them from the American Meteorite Laboratory, Denver, Colorado, U. S. A., They are $\sim$0.5 mm in diameter (U.S. Standard Screen Series #35 mesh) and have a mean weight of 0.39 mg [approximate count per gram of 2,535 (American Meteorite Laboratory catalogue)]. They were collected from an area about 3/4 mile northeast of the crater. They will be referred to as the small spheroids.

Another set was obtained directly from the American Meteorite Laboratory (Dr. G. I. Huss, Director). They are $\sim$1.18 mm in diameter (U. S. Standard screen series #16 mesh) and have a mean weight of 4.12 mg (see Table 25, Appendix I). Dr. Huss (personal communication) indicated that they were collected from the area one to three miles northeast of the crater rim. They will be referred to as the medium spheroids.

A third set was obtained from Dr. C. B. Moore, Director, Arizona State University for Meteorite Studies. They have a mean weight of 4.91 mg (see Table 26, Appendix I) but their mesh number and original location are not known by the author. If it is assumed they have a mean density identical to the medium spheroids then their diameter may be calculated to be $\sim$1.25 mm. They will be referred to as the large spheroids.

B. Whole Spheroid Measurements

The $\delta^{34}S$ values of the spheroids were measured to discover if any isotope fractionation has occurred either during or after their formation. The three sets of spheroids described in the previous section were analysed to see if the $\delta^{34}S$ values or sulphur concentrations varied with spheroid size. The sulphur concentrations were measured as described in Chapter 2, Section B.3, and the Ag_2S produced was converted into SF_6 for $\delta^{34}S$ measurements as described in Chapter 2, Sections B.4 and C.1. The results are summarized in Table 3 and 4 and are given in detail in Appendix II.

The difference between the mean sulphur content of the medium spheroids and the large spheroids is not significant, being (0.026 $\pm$ 0.021) weight percent whereas the mean sulphur content of the small spheroids differs from

TABLE 3

SUMMARY OF WHOLE SPHEROID SULPHUR CONTENT MEASUREMENTS

Sample Type	Weight % sulphur Mean and standard deviation of the mean [standard deviation of the individual sample]	Weight % sulphur Lowest value	Weight % sulphur Highest value
Small (~323 spheroids per sample)	0.825 ± 0.012 ($\pm 1.45\%$) [± 0.045 ($\pm 5.43\%$)] 14 samples	0.731	0.921
Medium (~24.8 spheroids per sample)	1.005 ± 0.017 ($\pm 1.73\%$) [± 0.070 ($\pm 6.97\%$)] 17 samples	0.860	1.102
Large (~22.08 spheroids per sample)	0.979 ± 0.012 ($\pm 1.61\%$) [± 0.043 ($\pm 5.80\%$)] 13 samples	0.859	1.059

TABLE 4

SUMMARY OF $\delta^{34}S$ (CANYON DIABLO STANDARD) VALUES FOR THE WHOLE SPHEROID SAMPLES

Sample type	Mean and standard deviation of the mean ($\delta^{34}S$ ‰)	[1] Standard deviation of an individual measurement (‰)	[2] Standard deviation for an individual spheroid (‰)
Small (~323 spheroids per sample)	+0.400 $\pm$0.044 14 samples	$\pm$0.165	$\pm$2.97
Medium (~24.8 spheroids per sample)	+0.226 $\pm$0.035 17 samples	$\pm$0.144	$\pm$0.717
Large (~22.08 spheroids per sample)	+0.217 $\pm$0.038 13 samples	$\pm$0.137	$\pm$0.644

[1] Standard deviation of the mean multiplied by the square root of the number of samples.

[2] Standard deviation of an individual measurement multiplied by the square root of the number of spheroids per sample.

the mean sulphur content of the large spheroids by (0.154 $\pm$ 0.017) weight percent. The large spheroids have about 1.2 times the sulphur content of the small spheroids.

Any intrinsic variations in the spheroid sulphur contents are masked by the variations in the chemical extraction procedure. For homogeneous material the standard deviation of an individual measurement is $\pm$4.36% (see Table 1) whereas the standard deviation of an individual spheroid sample measurement is $\pm$0.070% or $\pm$6.97% (see Table 3).

F. G. Hawley (Nininger, 1956), using wet chemical techniques, analysed one sample of 520 Canyon Diablo metallic spheroids having a mean weight of 3.61 mg per spheroid. The value obtained, 0.96% sulphur by weight, is in agreement with that of the present work, (1.005 $\pm$ 0.017)% for the #16 spheroids having a mean weight of 4.12 mg per spheroid.

The difference between the mean $\delta^{34}S$ value of the medium spheroids and the large spheroids is not signifcant, being only (0.009 $\pm$ 0.052)‰ whereas the mean $\delta^{34}S$ value of the small spheroids differs from the mean $\delta^{34}S$ value of the medium spheroids by a significant amount, (0.174 $\pm$ 0.056)‰.

Since the standard deviation of an individual measurement derived from identical Ag_2S sample $\delta^{34}S$ measurements (see Section C.2, Chapter 2) is only $\pm$0.0343‰ for this set of samples, almost all of the variation shown by the

$\delta^{34}S$ values is due to the $\delta^{34}S$ variations of the spheroid samples themselves. If a Gaussian distribution is assumed and the square root of the number of spheroids per sample is multiplied by the standard deviation of an individual measurement then the standard deviation for the individual spheroids may be obtained. These results are also shown in Table 4. The value for the small spheroids is ± 2.97 ‰ which is about four times that for the #16 spheroids and about 4.6 times that for the largest spheroids. This implies that there would be some small spheroids with $\delta^{34}S$ values as great as [+0.400 + 2(2.97)]‰ or +6.34‰ and as low as [+0.400 - 2(2.97)]‰ or -5.54‰. It should be noted that there is a suggestion of a skewed distribution for the $\delta^{34}S$ values of the #35 spheroids as there are only 5 samples with $\delta^{34}S$ values greater than the mean compared to 9 samples with $\delta^{34}S$ values less than the mean. This is in contrast to the sulphur content values which have very nearly equal numbers of values greater than or less than the mean. However, as pointed out previously, the experimental error in the sulphur content data masks any intrinsic variations.

C. Ablated Spheroid Measurements

Measurements of the sulphur concentrations and $\delta^{34}S$ values as they vary with depth within the spheroids were carried out because of the following observations. Mead, Littler and Chao (1965) describe the spheroids as being coated with a brown iron oxide layer. They also observe that directly beneath this layer, most if not all, of the spheroids have a fragile thin white coating of silica or silica glass containing numerous angular fragments of quartz. Beneath this layer they commonly found a layer of grey iron oxide surrounding the core of metallic nickel iron. Also, F. G. Hawley (Nininger, 1956) found by removing the oxide crust that the chemical composition of the spheroid cores was different from that of the spheroids as a whole (see Table 5). In order to investigate the variations with depth of sulphur content and $\delta^{34}S$ values a series of ablations on samples of spheroids was undertaken.

For each ablation series 200 spheroids, all from either the medium or large group, were weighed and placed in a ceramic vial of about 100 cc capacity. The vial was then agitated in an automatic mixer/mill (Spex Industries, Inc., Scotch Plains, N. J., Catalogue #8000) for a 3-hour period. As the spheroids rubbed against the side of the vial their outer surfaces were ground off to form a fine

TABLE 5

WET CHEMICAL ANALYSIS BY F. G. HAWLEY

OF CANYON DIABLO METALLIC SPHEROIDS

(after Nininger, 1952, p. 242)

Description of component	Total sample (% weight)	Metallic portion (% weight)
Fe	53.88	75.63
Ni	9.06	17.30
Co	0.95	2.22
P	0.56	not determined
S	0.96	not determined
CaO	1.10	not determined
Insoluble residue	16.10	1.15
Calculated oxygen	7.96	not determined
H_2O	7.00	not determined
Total	97.57	96.30

powder. The dust tended to cling to the walls of the vial but was removed using small brushes and weighed. The ablated spheroids were washed in acetone (to remove any dust clinging to them) dried and weighed. The vial was cleaned with tissues until no more dust could be removed. The spheroids were returned to the vial and the whole ablation, weighing and cleaning procedure repeated until five separate fractions were collected. The non-dust residue consisted of rounded spheroid cores of various sizes and some relatively small irregular chips or fragments. The spheroid cores were separated into four samples of approximately equal mass. The largest ones were isolated first, followed progressively by the smaller ones. This size-separation by eye was carried out to discover if there was any trend of sulphur content or $\delta^{34}S$ values with core size. The details of each separation are given in Appendix III. The fragments were treated as a separate sample. The sulphur concentrations and $\delta^{34}S$ values were measured as described in Sections B.3, B.4, C.1 and C.2, of Chapter 2. The results are shown in detail in Appendix III and a summary is shown in Tables 6, 7, 8 and 9. A diagram schematically summarizes the results in Fig. 5.

The observations of Mead, Littler and Chao (1965) and F. G. Hawley (Nininger, 1952) concerning the existence

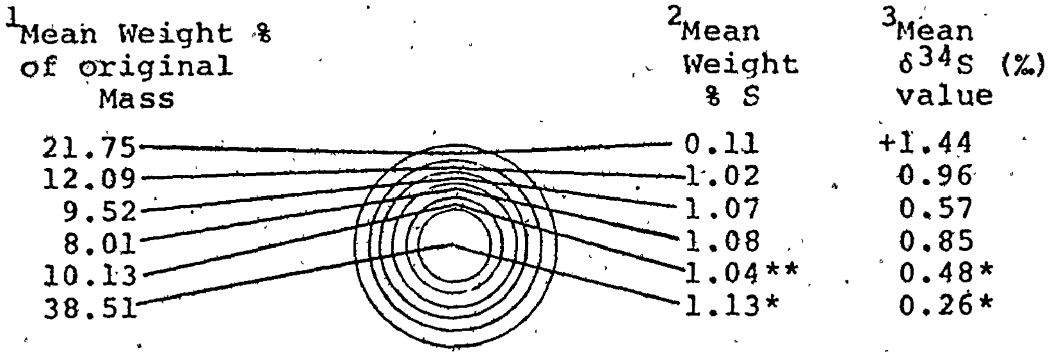

Medium
Spheroids

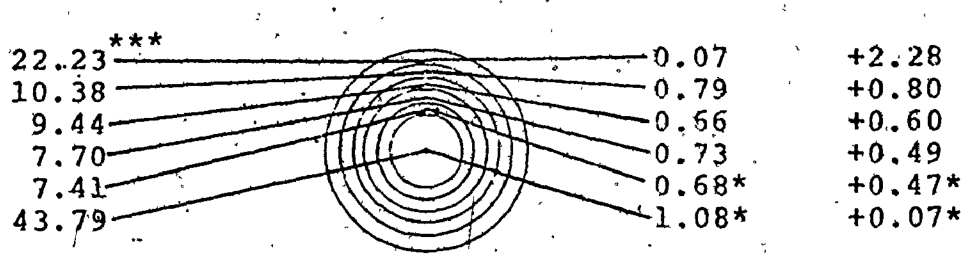

Large
Spheroids

[1]Calculated from the data in Table 10.

[2]Calculated from the data in Tables 6 and 8.

[3]Calculated from the data in Tables 7 and 9.

*Mean of spheroid core samples excluding the fragments.

**Excluding the 2.04% value.

***First and second layer samples of Series #1 added together and averaged with the 1st layer sample from Series #3.

Figure 5. Schematic Representation of the Ablated Spheroid Results

TABLE 6

[1]WEIGHT % SULPHUR OF THE ABLATION SAMPLES
FROM THE MEDIUM SPHEROIDS

Sample type	[2]Series #4	[2]Series #5	[2]Series #6	[3]Percent Mass
1st layer	lost	0.11	0.10	20.09
2nd layer	lost	0.97	1.06	11.41
3rd layer	1.09	1.01	1.12	9.49
4th layer	1.00	0.96	1.29	7.89
5th layer	0.96	1.12	2.04	9.04
Largest ablated spheroids	1.18	1.24	1.17	11.71
2nd largest	1.32	1.15	[4]0.97	10.19
3rd largest	1.15	1.09	1.15	9.75
4th largest	1.10	1.04	0.96	6.81
Fragments	0.97	0.92	0.93	2.69

Mean sulphur content of ablated spheroids, excluding the fragments, and standard deviation of the mean is (1.126 $\pm$ 0.030) weight percent.

[1]Standard deviation of an individual sample is approximately $\pm$0.04% (see Table 1).

[2]The layer sample values were corrected for lost dust by assuming a homogeneous sulphur content.

[3]From Table 10.

[4]Possible loss of Ag_2S due to shattering of the centrifuge tube.

$$(1.126 \pm 0.030) - (1.084 \pm 0.0227) = 0.042 \pm 0.038.$$

TABLE 7

$\delta^{34}S$(‰) VALUES OF THE ABLATION SAMPLES FROM THE MEDIUM SPHEROIDS

Sample type	Series #4	Series #5	Series #6	[2] Approximate % of total sulphur
1st layer	lost	+1.66	+1.22	1.87
2nd layer	lost	+1.02	+0.71	10.25
3rd layer	+0.84	+0.57	+0.31	9.27
4th layer	+0.85	lost	lost	6.40
5th layer	+0.67	+0.04	+0.72	4.89
Largest ablated spheroids	+0.21	+0.06	+0.46	20.32
2nd largest	+0.15	+0.07	lost	17.95
3rd largest	+0.33	+0.32	+0.32	16.06
4th largest	+0.20	+0.16	+0.55	8.44
Fragments	+0.47	+0.38	+0.31	4.57

[1] Standard deviation of an individual measurement is ±0.06‰.

[2] From Table 11.

TABLE 8

[5]WEIGHT % SULPHUR OF THE ABLATION SAMPLES FROM THE LARGE SPHEROIDS

Sample type	[1]Series #1	[3]Series #2	[1]Series #3	[2]Percent mass
1st layer	[4]0.07	0.04	0.10	20.09
2nd layer	[4]----	0.71	0.86	11.41
3rd layer	0.53	0.58	0.88	9.49
4th layer	0.75	0.63	0.82	7.89
5th layer	0.73	0.57	0.73	9.04
Largest ablated spheroids	lost	1.11		11.71
2nd largest	lost	1.13	1.18	10.19
3rd largest	1.16	1.06	1.10	9.75
4th largest	1.01	1.02	0.99	6.81
Fragments	1.00	1.09	0.93	2.69

Mean sulphur content of ablated spheroids excluding the fragments and standard deviation of the mean is (1.084 $\pm$ 0.0227) weight %.

[1]The layer sample values were corrected for lost dust by assuming a homogeneous sulphur content.

[2]From Table 10.

[3]The layer samples were not corrected for lost dust since the amount lost was not recorded.

[4]First two layer samples were combined.

[5]Standard deviation of an individual sample is approximately $\pm$0.04% (see Table 1).
(1.084 $\pm$ 0.0227) - (0.979 $\pm$ 0.012) = 0.105 $\pm$ 0.026 (quadratic addition of standard deviations). Also, (1.126 $\pm$ 0.030) - (1.005 $\pm$ 0.017) = (0.121) $\pm$ 0.034).

TABLE 9

$\delta^{34}S$ (‰) VALUES OF THE ABLATION SAMPLES

OF THE LARGE SPHEROIDS[1]

Sample type	Series #1	Series #2	Series #3	[2]Approximate % of total sulphur
1st layer	+2.20	+2.60	+2.04	1.87
2nd layer	lost	+0.84	+0.76	10.25
3rd layer	+0.62	+0.40	+0.79	9.27
4th layer	+0.62	+0.08	+0.76	6.40
5th layer	+0.64	+0.15	+0.61	4.89
Largest ablated spheroids	lost	-0.12	-0.10	20.32
2nd largest	lost	-0.08	-0.04	17.95
3rd largest	-0.09	0.00	+0.36	16.06
4th largest	+0.04	+0.11	+0.58	8.44
Fragments	+0.45	+0.69	+0.41	4.57

[1]Standard deviation of an individual measurement is ±0.06‰.

[2]From Table 11.

of an oxide crust and silica coating are consistent with the following observations made during the course of this work. The dust collected from the first ablation appeared a dull red-brown in ordinary light and a dark yellow colour when dissolved in HCl, whereas the dust from the second and subsequent ablations appeared black in ordinary light and a light green colour when dissolved in the HCl. Jan Monster (Chemistry Dept., McMaster University)(private communication) has observed the dark yellow colour to be associated with iron (III) oxides while the green colour is associated with nickel. The observed layered structure is also consistent with the observation that although the first layer ablation material is representative of the outer ∿20% of the mass it contains only ∿2% of the total sulphur (see Table 10 and 11).

If the mean sulphur content of the cores (the ablated spheroids) is calculated (excluding the fragments) values of (1.126 $\pm$ 0.030) weight % and (1.084 $\pm$ 0.0227) weight % are obtained for the medium and large spheroids respectively (see Table 6 and 8). Using these values it is apparent that there is no significant difference between the medium and large spheroid cores (see the bottom of Table 6). However the sulphur contents of the cores are significantly different from that for the whole spheroids. For the large spheroids

TABLE 10

WEIGHT OF THE ABLATED SPHEROID SAMPLES
AS A % OF THE INITIAL SPHEROID WEIGHT

Sample type	Ablation Series Number 1	2	3	4	5	6	Mean
1st layer	14.05	[1]----	21.16	21.59	22.99	20.67	20.09
2nd layer	9.25	[1]----	11.50	11.37	12.49	12.42	11.41
3rd layer	9.07	[1]----	9.81	9.44	9.49	9.64	9.49
4th layer	8.02	[1]----	7.37	8.06	7.96	8.02	7.89
5th layer	8.53	[1]----	6.29	6.41	6.07	[2]17.91	9.04
Total layers	48.92	[1]----	56.13	56.87	59.00	68.66	57.92
Largest spheroids	12.60	15.66	12.49	10.40	10.48	8.60	11.71
2nd largest	12.61	10.25	10.99	9.59	9.77	7.95	10.19
3rd largest	12.05	8.57	10.54	10.29	9.39	7.68	9.75
4th largest	4.68	6.26	6.16	9.89	8.37	5.51	6.81
Fragments	2.53	2.43	3.56	2.91	3.07	1.62	2.69
Total spheroids and fragments	44.47	43.17	43.74	43.08	41.08	31.36	41.15
Overall Total	93.39		99.87	99.95	100.08	100.02	98.66

[1]Not recorded.

[2]Ablated for 5 hrs. 26 min., instead of 3 hours.

the difference is (0.105 $\pm$ 0.026) weight % sulphur while for the medium spheroids it is (0.121 $\pm$ 0.034) weight % sulphur (see bottom of Table 8).

The most striking observation is the difference in the sulphur content of the outermost layer and the next layer. Usually there is almost an order of magnitude difference between them.

The most striking observation on the $\delta^{34}S$ values is that the value for the outermost layer differs from the unaltered meteorite value of 0.0‰ by as much as +2.60 ‰. The standard deviation of an individual measurement is $\pm$0.0645‰ (determined as in Section C.2 of Chapter 2) so that these large values are certainly significant.

Each time an ablation was performed a fraction of the dust was lost during transfer from the vial to the weighing boat. In ablation series #3 and #5 none of the Ag_2S samples were lost so that corrections for the lost material could be performed as shown in Table 11 and Table 12. The assumption used in the calculations of the corrections was that the lost material had the same sulphur content as the material that was not lost. It should also be remembered that the material was lost from the outer portions of the spheroids which have a lower sulphur content than the inner portions. These two factors explain why the

TABLE 11

PERCENT OF TOTAL SULPHUR
IN EACH ABLATION SAMPLE TYPE IN SERIES #3

Sample type	Weight of Ag_2S actually collected (mg)	[1] Ag_2S weight corrected for dust lost (mg)	% of total sulphur
1st layer	0.60	0.99	1.87
2nd layer	4.04	5.43	10.25
3rd layer	3.79	4.91	9.27
4th layer	2.60	3.39	6.40
5th layer	1.99	2.59	4.89
Largest	10.77	10.77	20.32
2nd largest	9.51	9.51	17.95
3rd largest	8.51	8.51	16.06
Smallest	4.47	4.47	8.44
Fragments	2.42	2.42	4.57
Total	47.80	52.99	100.02

Original unablated spheroid sample weight = 0.95185 gm

Corrected weight % for whole sample = [2] 0.72%

Uncorrected weight % for whole sample = [3] 0.80%

[1] The layer samples were corrected for the known amount of dust that was lost assuming that the dust sample was homogeneous.

[2] Using the figures 52.99 mg and 0.95185 gm.

[3] Using 48.70 mg and the actual weight of the collected material.

TABLE 12

PERCENT OF TOTAL SULPHUR
IN EACH ABLATION SAMPLE TYPE IN SERIES #5

Sample type	Weight of Ag_2S actually collected (mg)	[1]Ag_2S weight corrected for dust lost (mg)	% of total sulphur
1st layer	0.41	0.77	1.84
2nd layer	3.17	4.75	11.38
3rd layer	2.90	4.03	9.66
4th layer	2.04	3.02	7.24
5th layer	1.38	2.34	5.61
Largest	7.60	7.60	18.21
2nd largest	6.54	6.54	15.67
3rd largest	5.97	5.97	14.30
Smallest	5.08	5.08	12.17
Fragments	1.64	1.64	3.93
Total	36.73	41.74	100.01

Original unablated spheroid sample weight = 0.75425 gm.

Corrected weight percent for whole sample = [2]0.72%.

Uncorrected weight percent for whole sample = [3]0.81%.

[1]The layer samples were corrected for the known amount of dust that was lost, assuming that the dust sample was homogeneous.

[2]Using the figures 41.74 mg and 0.75425 gm.

[3]Using 36.73 mg and the actual weight of the collected ablation material.

corrected sulphur content (0.72 weight %) from Table 11 is less than the uncorrected sulphur content (0.80 weight %).

As was just noted the corrections were performed with the assumption that the lost material had the same sulphur content as the material that was not lost. However, the Table 11 corrected sulphur content (0.72 weight %) is considerably lower than the lowest sulphur content observed for the whole spheroids (0.86 weight %). This strongly suggests that the lost material had a greater sulphur content than the material that was not lost. This is understandable since it was observed that the finer dust was lost much more readily than the coarser dust. Troilite is considerably more brittle than the nickel-iron matrix so that proportionately more of the finer material would have been troilite.

Two of the large spheroid whole samples have $\delta^{34}S$ values greater than the (+0.37‰) value for the total sample calculated from the percent total sulphur and $\delta^{34}S$ values data in Tables 9 and 11 so that the ablated spheroid results are not inconsistent with the whole spheroid results.

There is a suggestion of a trend from lesser to greater $\delta^{34}S$ values from larger to smaller cores (see particularly ablation series #3) but ablation series #4 and #6 are inconsistent with that suggestion.

Blau et al. (1973) used a microprobe to measure the sulphur content in the metallic cores of 14 spheroids in the size range 0.7 mm to 1.8 mm. They found the range of sulphur concentrations by weight to be from 0.9% to 2.8% with a mean and standard deviation of the mean of (1.6 $\pm$ 0.2)%. The largest sulphur content for the ablated spheroids in this work is 1.32% by weight for the second largest ablated spheroids of ablation series #4 and the smallest is the 0.96% for the 4th largest sample from ablation series #6. Since the yield of the acid hydrolysis method used here is ∿91% (see Table 2) a corrected value of 1.32% would be ∿1.45%, which is within the 1.6 $\pm$ 0.2% range found by Blau et al. It should be noted that the size range of Blau et al's spheroids was much broader than that of the present work which had been pre-sieved. Also, the largest spheroids used in the present work were ∿1.25 mm in diameter whereas, as already pointed out, some of Blau et al's spheroids were as large as 1.8 mm.

CHAPTER 4

THE TROILITE HEATING EXPERIMENTS

A. The Sulphur Isotope Effects Associated with the Oxidation of Troilite

Measurement of the sulphur isotope effect in troilite oxidation was undertaken because both Blau et al. (1973) and Kelly et al. (1974) have suggested that the spheroids were oxidized during their flight through the atmosphere after the impact of the meteoroid.

A preliminary low-temperature experiment was inadvertently begun when a piece of Canyon Diablo troilite was ground to a fine powder for some other experiment in December, 1971. The material was stored in a non-airtight container until October, 1974 when it was brought to the author's attention. This material is referred to as "weathered" troilite throughout the remainder of the thesis. Ten samples were separately treated with HCl to convert the sulphide sulphur to Ag_2S, as described in Section B.3 of Chapter 2. The Ag_2S samples were converted to SF_6 as described in Section B.4 of Chapter 2, and the $\delta^{34}S$ values were obtained as described in Sections C.1 and C.2 of Chapter 2. The results are shown in Table 13. It is apparent that there is some variation due to the weathering,

TABLE 13

SULPHIDE SULPHUR CONTENT AND [1] $\delta^{34}S$ VALUES FOR THE "WEATHERED" CANYON DIABLO TROILITE

Original sample weight (mg)	Weight of collected Ag_2S (mg)	Weight % sulphide sulphur	[2] $\delta^{34}S$ (‰)
2.83	3.55	16.23	+0.25
2.37	3.38	18.45	-0.04
4.12	6.31	19.82	+0.24
4.13	5.50	17.23	+0.07
0.86	1.57	23.62	+0.11
0.88	1.88	27.64	-0.04
1.99	3.36	21.85	-0.07
1.72	3.03	22.79	-0.12
1.56	4.16	34.50	-0.04
4.17	5.72	17.75	-0.24
Mean		21.99	+0.012
Standard deviation of the mean		± 1.77	± 0.04914
[3]Standard deviation of an individual determination		± 5.61	± 0.1554

$$[(0.1554)^2 - (0.11146)^2]^{\frac{1}{2}} = 0.10829$$

$$(100\%)\left(\frac{5.605}{21.99}\right) = 25.49\%$$

[1]Values were obtained by comparison with a secondary standard whose $\delta^{34}S$ values with respect to non-weathered Canyon Diablo troilite was well known.

[2]The experimental standard deviation of an individual determination is ± 0.11146 ‰.

[3]Standard deviation of the mean multiplied by the square root of ten.

but that it is relatively small ($\pm$0.11 ‰) and random. The mean $\delta^{34}S$ value is not significantly different from 0.0 ‰. There is a large variation in the sulphur content ($\sim\pm$25 %) and the sulphur content is considerably less than the 36.47 weight percent value of stoichiometric troilite. This is most likely due to a large amount of nickel-iron impurities originally contained in and around the troilite nodule.

The material was also found to contain elemental sulphur so that further measurements were made. Two other samples of the same "weathered" troilite first had their elemental sulphur converted to CuS as described in Section B.2 of Chapter 2. The CuS was then converted to Ag_2S and finally to SF_6 for $\delta^{34}S$ value measurements as described in Sections B.3, B.4, C.1 and C.2. After the elemental sulphur had been extracted the sulphide sulphur contents and $\delta^{34}S$ values were measured as before. The results are shown in Tables 14 and 15. In these two cases the elemental sulphur components have positive $\delta^{34}S$ values while the corresponding sulphide sulphur components have negative values. These results are not in complete agreement with previously reported work.

Lewis and Krouse (1969) immersed troilite powder samples in distilled water held at various temperatures for various periods of time and found that they could collect

TABLE 14

RESULTS FOR THE SULPHIDE SULPHUR EXTRACTIONS FROM "WEATHERED" CANYON DIABLO TROILITE SAMPLES FROM WHICH THE ELEMENTAL SULPHUR HAD BEEN REMOVED

Sample number	Original weight (gm)	Weight of Ag_2S collected (mg)	Weight % of sulphide sulphur in sample	[1] $\delta^{34}S$ (‰)
TWT1	0.02592	40.71	20.32	[3] −0.22
TWT2	0.03142	49.55	20.41	[2] −0.02

TABLE 15

RESULTS FOR THE CORRESPONDING ELEMENTAL SULPHUR EXTRACTIONS

Sample number	Original weight (gm)	Weight of Ag_2S collected (mg)	Weight % of elemental sulphur in sample	% of total sulphur which was elemental	[1] $\delta^{34}S$ (‰)
TWT1(EL)	0.02592	3.55	1.77	8.02	[3] +0.38
TWT2(EL)	0.03142	2.66	1.10	5.09	[3] +0.39

[1] Values were obtained by comparison with a secondary standard whose $\delta^{34}S$ value with respect to non-weathered Canyon Diablo troilite was well known.

[2] The experimental standard deviation of an individual determination is ± 0.11 ‰.

[3] The experimental standard deviation of an individual determination is ± 0.08 ‰.

elemental and sulphate sulphur as reaction products from the oxidation of troilite. They measured the isotopic composition of both products and the results are shown in Table 16. Their value of +0.9‰ for elemental sulphur should be compared to the value of ∿0.38‰ of the present work since in the latter case the troilite was stored at room temperature. Lewis and Krouse state that product SO_4^{-2} is ∿3.5 times more abundant than S^o so that the residue troilite should have a positive $\delta^{34}S$ value. This is contrary to the observations of the present work since the sulphide sulphur in the two samples from which the elemental sulphur had been removed have negative $\delta^{34}S$ values. However, the reactions may be different in the two experiments since the experimental conditions were considerably different. The troilite of Lewis and Krouse was totally immersed in water while the troilite of the present work was only exposed to the moisture in the air. Lewis (1967) states that dry FeS is probably oxidized about three orders of magnitude slower than wet troilite. Therefore there is a possiblity that a kinetic isotope effect occurs in the faster (wetter) case while a partial equilibrium isotope effect occurs in the slower (drier) case. It should also be kept in mind that the mean $\delta^{34}S$ value of the "weathered" troilite was not significantly different from zero so that not all of the "weathered" troilite material had oxidized to the same extent. Also,

TABLE 16

*$\delta^{34}S$ VALUES OF LOW-TEMPERATURE TROILITE OXIDATION PRODUCTS

(after Lewis and Krouse, 1969)

	*$\delta^{34}S$ (‰)	
Temperature (°C)	Elemental sulphur	Sulphate sulphur
0	+1.4, +1.5, +0.4	-1.5, -2.8
25	+0.9	-1.9, -1.5
60	+0.9, +0.5	-1.4, -1.7, -1.7
100	+0.1, +1.3	-0.5, -0.8, -1.7

*Measured with respect to the starting material.

there is no certainty that the elemental sulphur from the two samples corresponds to the sulphide sulphur from the same samples with which they were found to be physically associated. However, there are two of the "weathered" troilite samples that have $\delta^{34}S$ values which are positive and more than two standard deviations different from zero. This suggests that for those samples the reaction of Lewis and Krouse may have occurred.

Kelly et al. (1974) and Blau et al. (1973) both suggest that the spheroids were oxidized shortly after their shock-melt formation while they were still relatively hot. For this reason further experiments were carried out. Artificial troilite of size 100 mesh was obtained from Cerac/Pure Inc. of Butler, Wisconsin. A 50 g portion of lot #3841 arrived with an X-ray diffraction analysis report showing major FeS hexagonal (troilite) and a trace of cubic FeS plus possible traces of Fe and FeO.

The following precautions were carried out since the earlier experiments showed troilite would oxidize if left exposed to the atmosphere. The troilite arrived packed under dry argon and was then opened under an atmosphere of dry nitrogen in a glove bag. The major mass of the troilite was stored in its original bottle which was in turn stored inside another sealed bottle half-filled with $CaSO_4$. This second bottle was stored inside the glove-bag filled with dry nitrogen and containing an open bottle of $CaSO_4$. A small portion was stored in a dessicator for everyday use.

Samples of the Cerac artifical troilite were heated in dry air at ∿1200°C as described in Section A.3 of Chapter 2. Afterwards, the troilite residues were treated with HCl to yield Ag_2S as described in Section B.3 of Chapter 2. The product SO_2 was captured and converted to $BaSO_4$ and then to Ag_2S as described in Sections B.1 and B.3 of Chapter 2. The Ag_2S samples from both sources were then converted to SF_6 and the $\delta^{34}S$ values were measured as described in Sections B.4, C.1 and C.2 of Chapter 2. The results are shown in Tables 17 and 18. They are also shown in a graph in Figure 6.

It is apparent from the graph that there is no regular relationship between the $\delta^{34}S$ values and the extent of the reaction so that the mean values are used in the following discussion. The mean $\delta^{34}S$ value of the residue is significantly different from the mean $\delta^{34}S$ value of the product SO_2, being (0.66 ± 0.12)‰ or about 5.5 standard deviations. The mean $\delta^{34}S$ value of the residues is also significantly different from that of the starting material, the difference being (-0.33 ± 0.08)‰ or about four standard deviations. Also, the mean $\delta^{34}S$ value of the SO_2 is significantly different from that of the starting material being (0.33 ± 0.11)‰ or

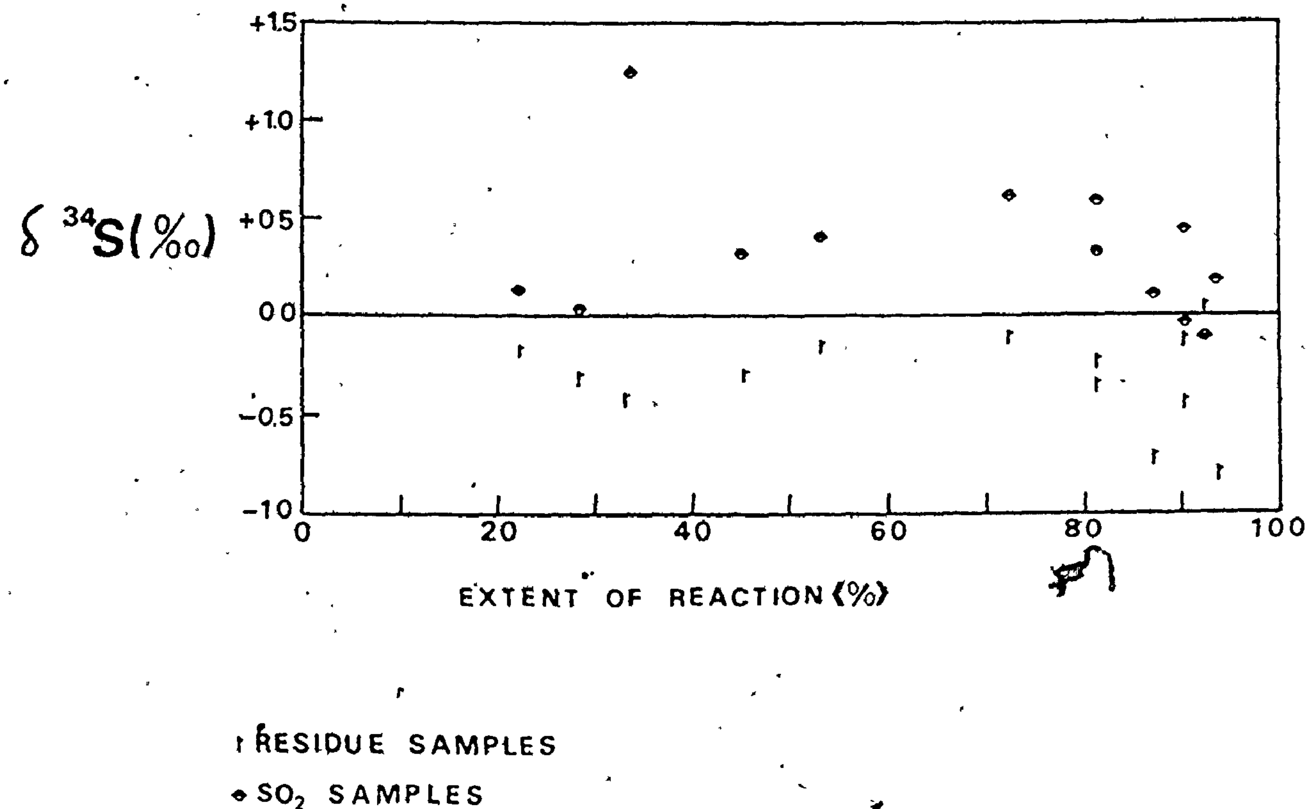

Figure 6. $\delta^{34}S$ Versus the Extent of Reaction for the High-Temperature Oxidation Data

TABLE 17

[1]SULPHUR CONTENTS

IN THE OXIDATION EXPERIMENT AT ∿1200°C

Sample number	Original sample weight (mg)	Ag_2S weight from residue (mg)	Ag_2S weight from SO_2 (mg)	% residue	% SO_2	% lost	Time in min. at ∿1200°C
12	13.54	20.70	4.51	55.02	11.99	32.99	5
13	9.28	11.07	4.30	46.84	16.68	36.48	5
17	21.83	43.34	1.02	71.46	1.68	26.86	2
27	37.07	68.66	6.58	66.66	6.39	26.95	12
28	54.38	117.55	0.57	77.80	0.38	21.82	2
31	6.74	1.82	9.17	9.72	48.97	41.31	12
35	9.53	4.92	4.35	18.58	16.43	64.99	15
36	3.41	2.65	1.56	27.97	16.47	67.10	2
40	6.63	1.40	9.68	7.60	52.55	39.85	10
41	7.28	3.86	6.63	19.08	32.78	48.14	10
42	9.11	1.64	7.44	6.48	29.39	64.13	25
43	10.18	3.74	9.24	13.22	32.67	54.11	20
44	10.57	2.90	7.09	9.87	24.17	65.99	24

[1]Based on 35.95 weight percent sulphur for the initial troilite. This is the value provided by Cerac/Pure Inc. and was obtained by spectrographic analysis.

TABLE 18

$^{1}\delta^{34}S$(‰) VALUES

IN THE OXIDATION EXPERIMENT AT ∿1200°C

Sample number	Residue component	SO_2 component	[2]% Extent of reaction
12	-0.31	+0.31	44.98
13	-0.17	+0.39	53.16
17	-0.31	+0.03	28.54
27	-0.44	+1.24	33.34
28	-0.19	+0.13	22.20
31	-0.10	-0.04	90.28
35	-0.32	+0.33	81.42
36	-0.11	+0.60	72.03
40	+0.04	-0.09	92.40
41	-0.50	+0.59	80.92
42	-0.79	+0.18	93.52
43	-0.72	+0.11	86.78
44	-0.43	+0.45	90.13
Mean, standard deviation of the mean	-0.3346 ±0.0669	+0.3254 ±0.0981	

$^{1}\delta^{34}S$ values are with respect to the initial troilite. The experimental standard deviation of an individual sample is ±0.18 ‰.

[2]Calculated from the data in Table 14.

0.3254 + 0.3346 = 0.66

Square root of $[(0.0669)^2 + (0.0981)^2] = \pm 0.12$.

about three standard deviations. The percentage of sulphur not recovered is considerable, ranging from ∿22% to ∿66%.

One possible source of loss of the SO_2 is that the following reaction takes place:

$$SO_2(g) + 1/2\ O_2(g) \rightleftarrows SO_3(g)$$

and SO_3 has a melting point of 16.8°C and a boiling point of 44.8°C, therefore most of the SO_3 produced would not be pumped out with the SO_2. However, the yield of SO_3 decreases rapidly with temperature and depends on the partial pressure of O_2 in the container so that at 1100°C with dry air the yield is ∿96% (Sakai and Yamamoto, 1966). The experiments of the present work were performed at a temperature of ∿1200°C so that it is apparent that the possible loss from this reaction is small. However, there is an equilibrium isotope effect involved in the formation of SO_3 which concentrates the ^{34}S in the SO_3 so that the SO_2 is isotopically lighter than it would be otherwise. Sakai and Yamamoto (1966) provide a value of 4.5×10^{-3} for α, (K-1), at 1100°C so that the $\delta^{34}S$ values of the SO_2 samples should have a relatively small value of about +0.18‰ added to them to offset the effect of the SO_3 formation.

The large percentages of the sulphur not recovered are most likely due to mechanical losses of $BaSO_4$ which may have occurred during the filtering and collection processes.

However, the mechanisms of sulphur loss, whatever they may be, must not have had large isotope fractionation effects associated with them since the $\delta^{34}S$ values of the lost material (calculated from the isotope mass balance equation) are close to zero. These calculated values are shown in Table 19. The standard deviations of the calculated values are relatively large and vary from sample to sample.

The isotope effect observed in this high-temperature, dry-air experiment is such that the residue samples have negative $\delta^{34}S$ values with respect to the initial troilite. The calculated isotope effect of troilite heated in water (the Lewis and Krouse experiment) is such that the residue samples have positive $\delta^{34}S$ values with respect to the initial troilite.

TABLE 19

CALCULATED $\delta^{34}S$ VALUES

FOR THE LOST MATERIAL IN THE OXIDATION EXPERIMENT

[1]$\delta^{34}S$(‰) for SO_2	Fraction SO_2	[1]$\delta^{34}S$(‰) for residue	Fraction residue	Fraction lost	[1]Calculated $\delta^{34}S$(‰) for lost material
[2]+0.49	0.1199	-0.31	0.5502	0.3299	-0.34
+0.57	0.1668	-0.17	0.4684	0.3648	+0.04
+0.21	0.0168	-0.31	0.7146	0.2686	-0.81
+1.42	0.0639	-0.44	0.6666	0.2695	-0.75
+0.31	0.0038	-0.19	0.7780	0.2182	-0.67
+0.14	0.4897	-0.10	0.0972	0.4131	+0.14
+0.51	0.1643	-0.32	0.1858	0.6499	+0.04
+0.78	0.1647	-0.11	0.2797	0.6710	+0.15
+0.09	0.5255	+0.04	0.0760	0.3985	+0.13
+0.77	0.3278	-0.50	0.1908	0.4814	+0.33
+0.36	0.2939	-0.79	0.0648	0.6413	+0.09
+0.29	0.3267	-0.72	0.1322	0.5411	0.00
+0.63	0.2417	-0.43	0.0987	0.6599	+0.17
Mean, standard deviation of the mean					-0.11 $\pm$0.11

[1]With respect to the initial troilite.

[2]All of the SO_2 samples were corrected for the formation of SO_3 (see text).

B. The Sulphur Isotope Effects Associated with the Vacuum Heating of Troilite

1. Introduction to this Section and a Short Review of the Experimental Procedures

Both H. H. Nininger (1956) and P. Ramdohr (1966) have suggested that the Canyon Diablo metallic spheroids condensed from the center of a metal-vapour cloud so that they were not exposed to the atmosphere until after they solidified. The sulphur isotope fractionation occurring during the dissociation of troilite in an oxygen-free environment was determined experimentally in order to see whether the isotope pattern observed in the spheroids is compatible with such a mode of formation.

The Cerac artificial troilite used in these experiments was the same as that used in the previously described oxidation experiments. The following description of the experimental procedure is essentially the same as that given in Section A.2 of Chapter 2. However, it is presented here for the sake of convenience and clarity.

In each experiment a troilite sample was weighed and placed in the end of a quartz tube which was then attached to a vacuum system and evacuated (see Fig. 2). In order to ensure the removal of air and water vapour the samples were pumped on overnight. Dry ice was placed around the

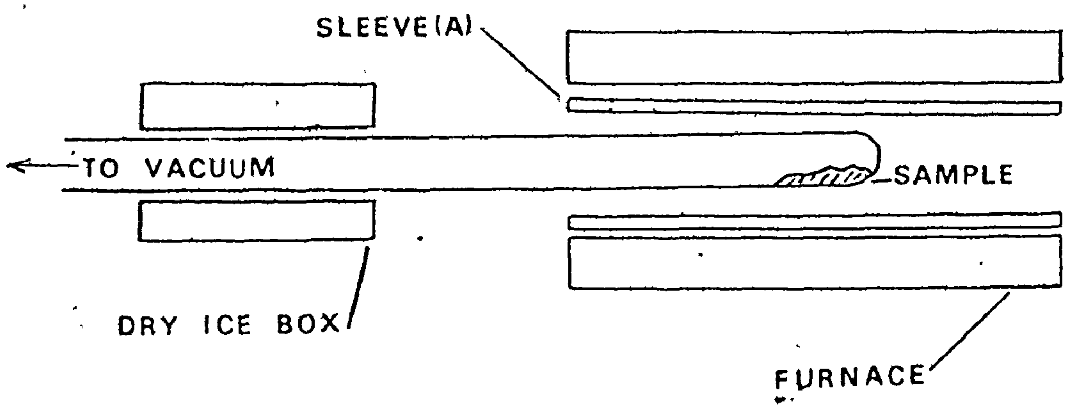

Figure 2. Schematic Diagram of the Dissociation/Evaporation Apparatus

quartz tube, as indicated in Fig. 2, to condense sulphur, and the furnace surrounding the troilite sample was heated to an indicated temperature of 1100°C for a predetermined length of time after which the sample was cooled by removal of the furnace. As mentioned in Section A.2 of Chapter 2 the actual temperature of the troilite itself must have been about 1200°C. The cooled tube was broken into two sections, one containing the elemental sulphur and the other containing the residual troilite. Elemental sulphur was converted to CuS using a Soxhlet apparatus as described in Section B.2 of Chapter 2. The CuS and residual troilite were in turn converted to Ag_2S, for weighing, as described in Section B.3 of Chapter 2 and then to SF_6, for mass spectrometric analysis, as described in Sections B.4, C.1 and C.2 of Chapter 2. The results of these measurements are shown in Table 20.

It was observed that there was a cylindrical ring, having a shiny, metallic lustre, coating part of the inside of the tube section containing the elemental sulphur. The elemental sulphur condensed in the tube region cooled by the surrounding dry ice, whereas the shiny material condensed in the intermediate temperature region about halfway between the edge of the furnace and the edge of the dry ice container. The quantity of this material appeared

TABLE 20

INITIAL MEASURED DATA IN THE DISSOCIATION EXPERIMENT

Sample number	Heating time (hours)	Sample weight (g)	Weight Ag_2S from residue (g)	Weight Ag_2S from dissociated sulphur (g)	Residue [1] $\delta^{34}S$ (‰)	Dissociated sulphur [1] $\delta^{34}S$ (‰)
1	0.5	0.06540	0.17013	0.00148	+ 0.44	-11.65
2	1.5	0.08490	0.21164	0.00957	+ 0.81	-14.13
3	10	0.07345	0.16708	0.02027	+ 2.13	-12.54
4	4	0.05240	0.11806	0.01517	+ 2.01	-13.40
5	2	0.00322	0.00577	0.00140	+ 4.04	-12.09
6	4	0.00650	0.00911	0.00323	+ 4.51	- 9.93
7	4	0.00360	0.00360	0.00154	+ 5.84	- 9.91
8	3	0.00169	0.00133	0.00112	+ 9.58	- 8.36
9	3	0.00218	0.00169	0.00150	+ 9.55	- 8.93
10	3	0.00142	0.00086	0.00069	+10.62	- 8.12

[1] With respect to the starting troilite.

to be relatively small so that no attempt was made at the time to extract any sulphur it may have contained. However, after preliminary study of the Table 20 data and a comparison of the experimental points with the theoretical curves for one-product and two-product reactions described below it became apparent that there must have been a second product of the reaction.

2. Equations Relating to One-and Two-Branch Reactions

The expressions governing first-order, one-step, one-and two-product reactions have been derived by Rees (1973) and Rees (unpublished) respectively. The time-independent expressions governing both types of reactions are shown for comparison and reference on page 73. The symbol A_o respresents the initial mass of the element of interest in the starting material and A, B, C represent the masses of the element of interest in the residue (reactant) and product (s) respectively after a fractional extent of reaction, f , has occurred. The symbols J, K and d represent first-order reaction rate constants, and P represents the branching ratio. The symbols α, b and g are the ratios of the rate constants for the different isotope species minus one. They are commonly referred to as "isotope effects" and are usually expressed in ‰. The δ values are measured with respect to the starting material. Equation 9 is the isotopic mass balance equation and equation 10 is the ordinary mass balance equation. In the derivations it is assumed that throughout the course of the reaction the branching ratio does not change and the reactant (residue) is well-mixed.

Time-independent expressions concerning both one-product and two-product reactions.

One-product reaction:

$$A \ \delta_A \xrightarrow{J,\alpha} B \ \delta_B$$

$$\frac{A}{A_o} = 1-f \quad \ldots\ldots \quad (1)$$

$$\delta_A = -\alpha \ \mathrm{Ln}(1-f) \quad \ldots\ldots \quad (2)$$

$$\delta_B = \alpha\left(\frac{1-f}{f}\right) \mathrm{Ln}(1-f) \quad \ldots\ldots \quad (3)$$

Two-product reaction:

$$\begin{array}{l} A \ \delta_A \xrightarrow{K,b} B \ \delta_B \\ A \xrightarrow{d,g} C \ \delta_C \end{array}$$

$$\frac{A}{A_o} = 1-f \quad \ldots\ldots \quad (4)$$

$$P = \left(\frac{d}{K}\right) = \left(\frac{C}{B}\right) \quad \ldots\ldots \quad (5)$$

$$\delta_A = \left(\frac{b+Pg}{1+P}\right) Ln(1-f) \qquad (6)$$

$$\delta_B = \left(\frac{b+Pg}{1+P}\right)\left(\frac{1-f}{f}\right) Ln(1-f) - \frac{P}{1+P}(b-g) \qquad (7)$$

$$\delta_C = \left(\frac{b+Pg}{1+P}\right)\left(\frac{1-f}{f}\right) Ln(1-f) + \frac{1}{1+P}(b-g) \qquad (8)$$

$$\delta_A A + \delta_B B + \delta_C C = \delta_{A_o} A_o = 0 \qquad (9)$$

$$A_o = A + B + C \qquad (10)$$

3. Further Discussion and Analysis of the Data

Particular graphs of the one- and two-branch equations governing the relationships between the δ values and the extent of reaction are shown in Fig. 7. The actual curves shown are for $\delta^{34}S$(‰) values versus the extent of reaction in %. Curves 2 and 3 are graphs of the one-product equations 2 and 3 where α equals 13‰. Curves 5, 7 and 8 are graphs of the two-product equations 6, 7 and 8 where g equals 13‰, b equals 5‰, and P equals one. The reason those particular values were used will be stated below.

For the one-product reaction, as the extent of reaction approaches 100% the $\delta^{34}S$ values of the residue approaches infinity and the $\delta^{34}S$ values of the product approaches zero. Such a process, where complete separation of two components is possible, is usually referred to as a

Rayleigh process after Lord Rayleigh who first discussed similar processes (Lord Rayleigh, 1896).

In a two-product reaction the $\delta^{34}S$ value of the residue also approaches infinity as the extent of reaction approaches 100%. The $\delta^{34}S$ value for one of the products changes sign before 100% extent of reaction occurs unless g equals b or g and b have opposite signs. The change of sign is evident in curve 7.

The data for the points shown in Fig. 7 was derived from the Table 20 data and an assumed sulphur content of 35.95 weight % for the starting troilite. (Discussion of the sulphur content of the starting troilite follows.) The $\delta^{34}S$ value error bars are too small to be shown on the figure since the standard deviation of an individual determination is ± 0.08 ‰. The values of α, g, b and P were chosen to approximately give the best fit to the points.

It is evident that the data points fit the residue and dissociated sulphur two-product curves better than they fit the corresponding one-product curves. (At this time none of the second-product data had been derived so that no fit with the second product curve (7) could be attempted.) The following considerations show that the data points are not

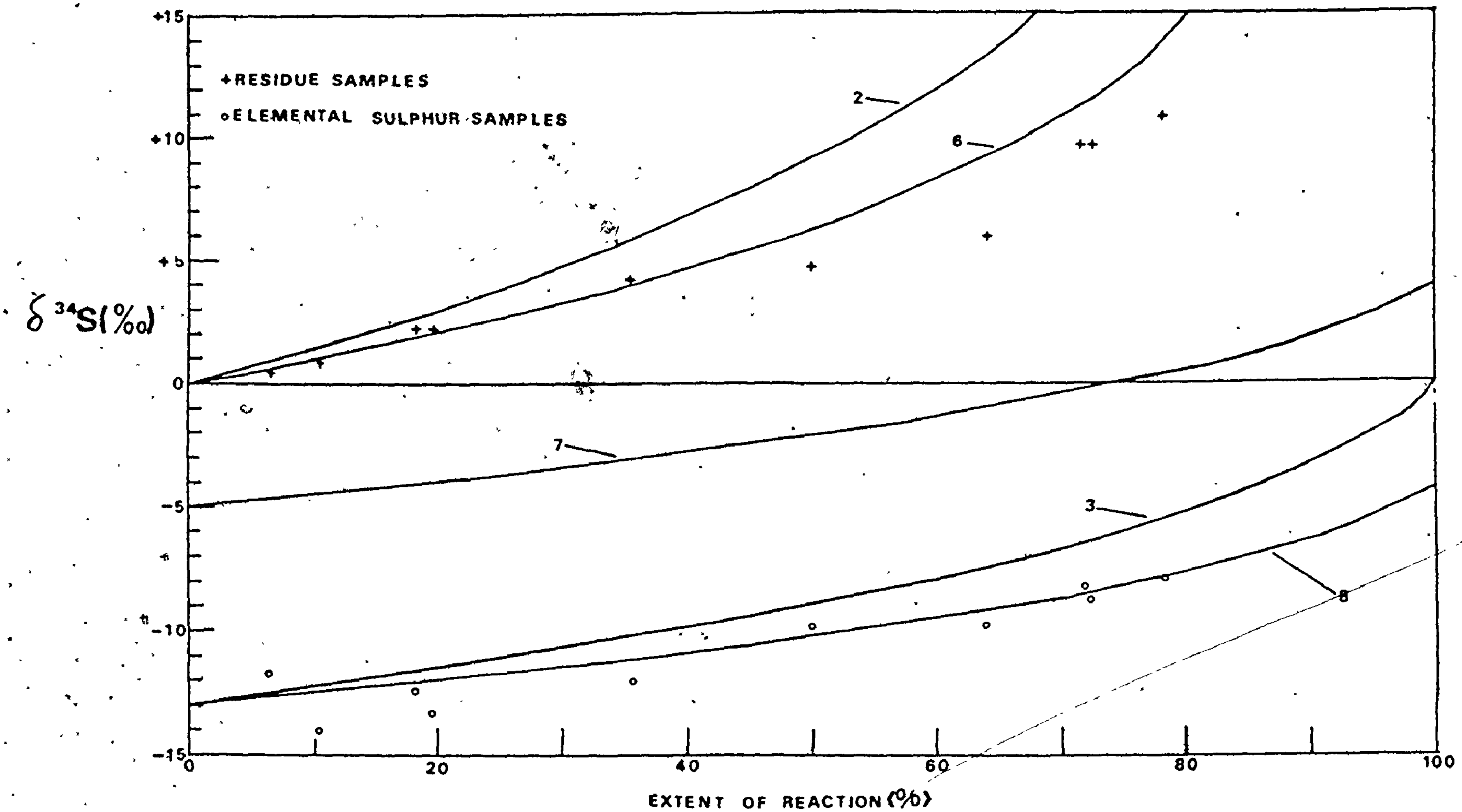

Figure 7. $\delta^{34}S$ Versus Extent of Reaction for One- and Two-Branch Reactions

compatible with the curves for a one-product reaction. An increase in the value of α moves the residue curve (2) farther from most of the residue points while a decrease in the value of α moves the dissociation curve (3) farther from most of the dissociated sulphur points.

It is evident from equations 4 to 6 that if either the quantity of the second product or the sulphur content of the starting troilite were known then the $\delta^{34}S$ values of the second product and the isotope effects g and b could all be calculated using the data of Table 20. Although Cerac/Pure Inc. provided a value of 35.95 weight % (obtained spectrographically) for the troilite it may not be correct. The greatest sulphur content obtained experimentally up to the time of these experiments was 33.66 weight % sulphur (see Table 2, page 24). Also, some Ag_2S is lost during each extraction so that a value for the quantity of the second product calculated from the data of Table 20 and a particular sulphur content would be somewhat uncertain. However, a large assumed sulphur content implies that more Ag_2S was lost than may have been the case while a small assumed sulphur content implies that less Ag_2S was lost than may have been the case. This allows an investigation of both factors, sulphur content and amount of Ag_2S lost, by only varying the assumed sulphur content. The quantities $\delta^{34}S$

for the second product, g and b were calculated using the data of Table 20 for three different sulphur contents in order to investigate their sensitivity to these variations. The results are shown in Tables 21 and 22. The value of 36.47 for sulphur, the weight % sulphur content of the starting troilite, was chosen because it is the value for pure stoichiometric troilite. The value for sulphur of 35.95 was used since Cerac/Pure Inc. provided it from spectrographic data. The value of 34.18 for sulphur was chosen for reasons which will be discussed below. It is apparent from Tables 21 and 22 that the calculated values of b and $\delta^{34}S$ values of the second product are more sensitive to the assumed sulphur content than are the calculated values of g. Also, the calculated values for samples 1, 2 and 3 were more sensitive than those for the other samples. At this point it was decided that the previously described shiny rings were probably troilite which had evaporated in the furnace and recondensed in the cooler region of the tube and that these troilite rings were in fact the second product. The rings could not be recondensed iron because the vapour pressure of elemental iron is only 1.3×10^{-14} atmospheres at 1273°C (Hultgren et al., 1963). Since the calculated values of the first three samples were observed to be the most sensitive to the assumed sulphur content (or amount of

TABLE 21

CALCULATED [1] $\delta^{34}S$(‰) VALUES FOR THE SECOND PRODUCT ASSUMING THREE DIFFERENT SULPHUR CONTENTS FOR THE STARTING TROILITE

Sample number	Calculated $\delta^{34}S$(‰) for the second product (S = 34.18)	Calculated $\delta^{34}S$(‰) for the second product (S = 35.95)	Calculated $\delta^{34}S$(‰) for the second product (S = 36.47)
1	-49.56	-5.70	-4.52
2	-11.74	-2.46	-2.00
3	-15.18	-6.07	-5.16
4	- 6.56	-2.75	-2.35
5	- 4.78	-3.59	-3.35
6	- 1.85	-1.56	-1.50
7	- 1.32	-1.18	-1.15
8	- 1.68	-1.48	-1.46
9	- 1.07	-0.96	-0.93
10	- 1.60	-1.47	-1.44

[1] With respect to the starting troilite.

TABLE 22

CALCULATED VALUES OF g AND b ASSUMING THREE DIFFERENT SULPHUR CONTENTS FOR THE STARTING TROILITE

Sample number	Calculated g (S=34.18)	Calculated g (S=35.95)	Calculated g (S=36.47)	Calculated b (S=34.18)	Calculated b (S=35.95)	Calculated b (S=36.47)
1	12.06	11.87	11.87	49.97	5.92	4.74
2	14.55	14.53	14.53	12.16	2.86	2.40
3	13.59	13.57	13.57	15.72	7.10	6.19
4	14.38	14.37	14.37	7.54	3.72	3.32
5	13.98	13.97	13.96	6.67	5.47	5.22
6	11.95	11.93	11.92	3.87	3.56	3.49
7	12.37	12.34	12.33	3.78	3.61	3.57
8	12.20	12.18	12.16	5.52	5.30	5.26
9	12.75	12.71	12.70	4.89	4.74	4.70
10	12.18	12.13	12.12	5.66	5.48	5.44
Mean	13.0	13.0	13.0	12	4.8	4.4
Standard deviation of the mean	±0.3	±0.3	±0.3	±4	±0.4	±0.4

Ag_2S lost) it was decided that the best test of the validity of the calculated values was to measure the quantities and $\delta^{34}S$ values of sulphur in the cylindrical troilite rings from the first three samples and compare the measured and calculated values.

The tube portions containing the shiny rings were treated with HCl in a reflux apparatus as described in Section B.3 of Chapter 2. The fact that they dissolved in HCl to produce H_2S showed that the rings contained sulphur in an acid soluble form. This supported the idea that the rings consisted of troilite which had evaporated. The Ag_2S samples were converted to SF_6 and the $\delta^{34}S$ values were measured as described in Sections B.4, C.1 and C.2 respectively. The results are shown in Table 23. The sum of the Ag_2S weights from the residue and the two products were used with the troilite sample weight to determine the apparent sulphur content of the starting material. The largest value so obtained was 34.18 weight % for sample 1. Since the true sulphur content must be greater than this (since some Ag_2S is undoubtedly lost) then this value was used in the previous calculations as a lower limit.

The values in the first two columns of Table 23 together with the data in Table 20 were used in equations (7) and (8) to calculate the values of g and b shown in the last two columns of Table 23.

TABLE 23

MEASURED DATA FOR THE SECOND PRODUCT

AND THE CORRESPONDING VALUES OF g AND b

	Weight Ag_2S from second product (g)	Measured [2]$\delta^{34}S$(‰) value of the recondensed troilite	[1]Calculated g (‰)	[1]Calculated b (‰)
1	0.00114	-5.21	11.72	5.28
2	0.00162	-3.87	14.46	4.20
3	0.00140	-5.36	13.31	6.13
Mean			13.2	5.2
Standard deviation of the mean			±0.8	±0.6

[1]Calculated using the measured values of this table and the data of Table 20.

[2]With respect to the starting troilite.

A comparison of the measured $\delta^{34}S$ values of the evaporated troilite with the calculated values of Table 21 indicates that the best choice of sulphur content is 35.95 weight %. A similar comparison of the g and b values of Table 23 with those of Table 22 is consistent with that conclusion.

In Table 24 there are two values for each quantity for the first three samples. One set of values were derived from the initial data without the benefit of the measurements on the evaporated troilite. The other set of values were derived using both the initial data and the additional data obtained from the measurements on the evaporated troilite. A comparison of these two values for the branching ratio, P, the extent of reaction, f, and the % of the total sulphur that evaporated as troilite shows that they differ considerably from one another. However, a further comparison of the corresponding values of g and b in Table 24 shows that they are in much closer agreement. This means that the quantities g and b are not relatively very sensitive to variations in the quantities P, f and the % of the total sulphur that evaporated as troilite.

All of these considerations provide confidence in the two-branch model and the calculated values of b and g. Two methods of obtaining a final value for g and b suggest

TABLE 24

A COMPARISON OF VARIOUS QUANTITY VALUES DERIVED BEFORE AND AFTER THE EVAPORATED TROILITE MEASUREMENTS

	% Residue	% Dissociated	% Evaporated	% Extent of reaction (f x 100)	Branching ratio (P)	g (‰)	b (‰)
1	93.6	0.8	5.6	6.4	0.1	11.87	5.92
*1	98.5	0.9	0.7	1.5	1.3	11.72	5.28
2	89.7	4.1	6.2	10.3	0.7	14.53	2.86
*2	95.0	4.3	0.7	5.0	5.9	14.46	4.20
3	81.4	9.9	8.2	18.1	1.2	13.57	7.10
*3	88.5	10.8	0.7	11.5	14.5	13.31	6.13
4	81.1	10.4	8.5	18.9	1.2	14.37	3.72
5	64.5	15.6	19.9	35.5	0.8	13.97	5.47
6	50.4	17.9	31.7	49.6	0.6	11.93	3.56
7	36.0	15.4	48.6	64.0	0.3	12.34	3.61
8	28.3	23.9	47.8	71.7	0.5	12.18	5.30
9	27.9	24.8	47.3	72.1	0.3	12.71	4.74
10	21.8	17.5	60.7	78.2	0.7	12.13	5.48

*These values were calculated using the measured evaporated troilite sulphur contents and their measured $\delta^{34}S$(‰) values.

themselves. Both use the values from Table 23 for samples 1, 2 and 3, but either the values calculated using 35.95 weight % or means of the values calculated using 34.18 weight % and 36.47 weight % might be used. The results using both of these methods are shown in Table 25. Although there is no significant difference between the means obtained by the two different methods perhaps it is preferable to use the 35.95 weight % derived results since the variation of b and g with assumed sulphur content is not linear. In summary, the kinetic isotope effect in the dissociation of troilite is $(+12.9 \pm 0.3)$‰ and the kinetic isotope effect in the evaporation of troilite is $(+4.8 \pm 0.3)$‰. In both cases the residue is enriched in ^{34}S relative to the products.

Fig. 8 shows two graphs each of the equations 6, 7 and 8 using different combinations of the following values for g, b and P for each graph. The values of P used are the smallest and largest from Table 24 (i.e. 0.1 and 14.5). The four values of g and b used are the Table 25 means, 12.9‰ and 4.8‰, plus or minus two standard deviations (i.e. $g + 2_\sigma$, $g - 2_\sigma$, $b + 2_\sigma$, $b - 2_\sigma$). The curves shown used the combinations of these six values of g, b and P which provided the greatest range of $\delta^{34}S$ values for each of the three equations.

TABLE 25

FINAL g AND b VALUES

Sample number	[1]g (‰)	[1]b (‰)	[2]g (‰)	[2]b (‰)
1	11.72	5.28	11.72	5.28
2	14.46	4.20	14.46	4.20
3	13.31	6.13	13.31	6.13
4	14.37	3.72	14.38	5.43
5	13.97	5.47	13.97	5.94
6	11.93	3.56	11.94	3.68
7	12.34	3.61	12.35	3.68
8	12.18	5.30	12.18	5.39
9	12.71	4.74	12.72	4.80
10	12.13	5.48	12.15	5.55
Mean	12.9	4.8	12.9	5.0
Standard deviation of the mean	±0.3	±0.3	±0.3	±0.3

[1]The values for samples 1, 2 and 3 are from Table 23, whereas those of 4 - 10 are from Table 22 where S = 35.95.

[2]The values for samples 1, 2, and 3 are from Table 23, whereas those of 4 - 10 are the mean values for S = 34.18 and S = 36.47 from Table 22.

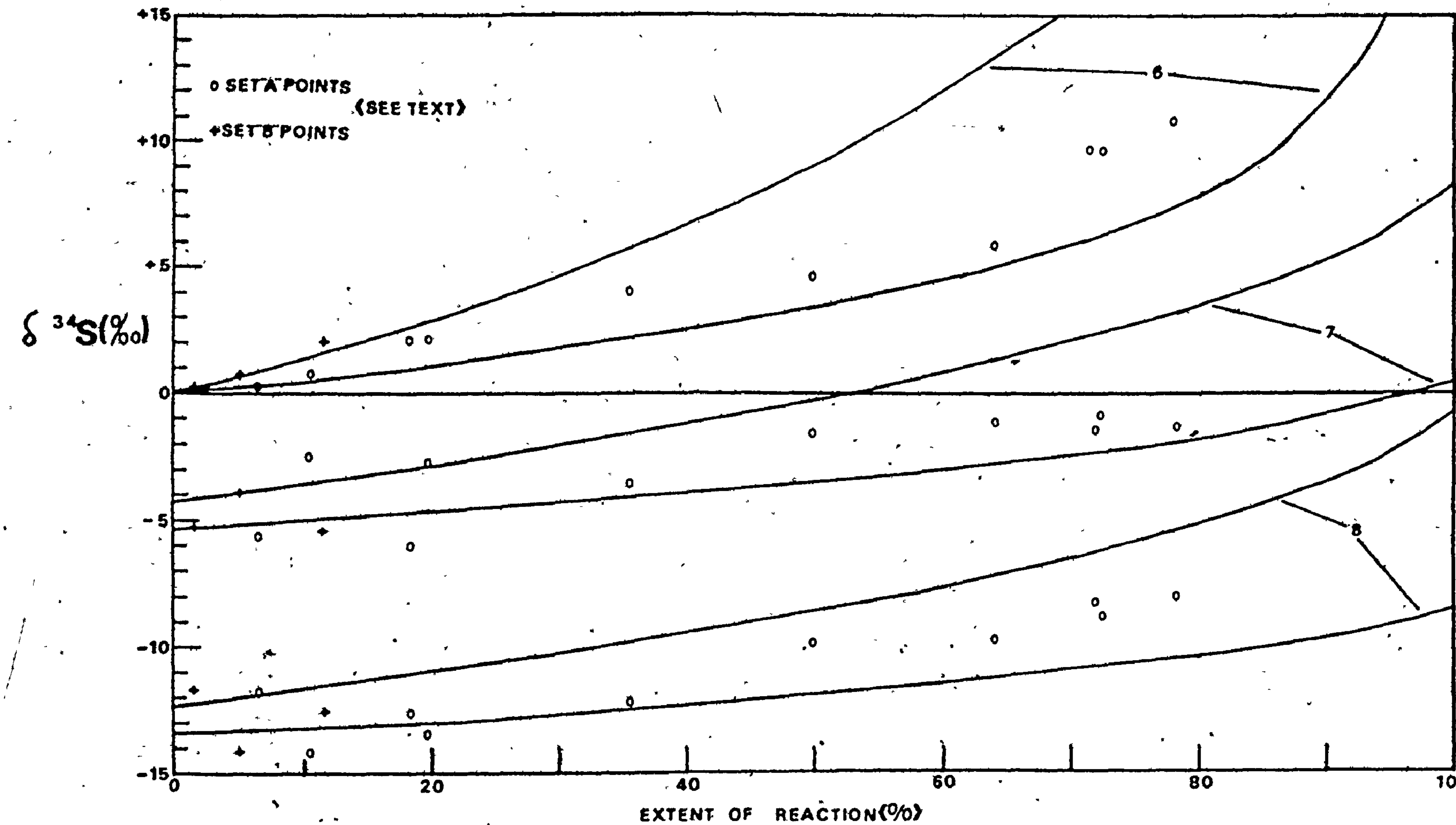

Figure 8. $\delta^{34}S$ Versus the Extent of Reaction for the Dissociation and Evaporation Data

Two sets of points are also shown in Fig. 8. One set (A) were derived from the Table 20 data (assuming a sulphur content of 35.95 weight % for the starting troilite). The other set of points (B) were derived from both the Table 20 data and the Table 23 data. The $\delta^{34}S$ error bars for the measured $\delta^{34}S$ values are too small to be shown since they represent plus or minus a standard deviation of an individual measurement of ± 0.08 ‰. The $\delta^{34}S$ value error bars for the calculated $\delta^{34}S$ values represent plus or minus a standard deviation for the individual sample.

The fact that only six of the points are outside of the regions defined by the corresponding curves is perhaps misleading. It would have been more appropriate (but a much less clear Fig. 8) if a region was drawn for each point corresponding to values of $g + 2_\sigma$, $g - 2_\sigma$, $b + 2_\sigma$, and $b - 2_\sigma$ and the value of P for that particular sample. This consideration means that the fit is not as good as it appears. However, in a general way the data does correspond to a two-product model. Some possible reasons for deviation from the two-product model are given below.

There was a different branching ratio for each sample and no correlation of this with any other factor could be found. This suggests the possibility of the branching ratio varying throughout the course of an individual sample reaction. The temperature may have varied across the sample since one side of it was in contact with its quartz glass container. The temperature itself may have varied somewhat from sample to sample. The temperature in the furnace was once checked with another thermocouple and a difference of ~50°C was found so that the temperature may have an uncertainty of ±50°C. The furnace temperature control needed frequent adjustment during the course of a reaction.

One of the assumptions in the equation derivations was that the troilite reactant (residue) be well-mixed during the course of the reaction. This apparently was the case since fairly good agreement is seen between the measured points and the theoretical graph curves. All residue samples showed indications of having been melted. Perhaps another possible source of error is that Cerac/Pure Inc. stated that their X-ray diffraction analysis showed a trace of cubic FeS whereas troilite is hexagonal FeS. However, in spite of all these possibilities the experiments as performed provide estimates, with rather narrow error limits, of the isotope effects in the dissociation and evaporation of troilite.

CHAPTER 5

DISCUSSIONS AND CONCLUSIONS

A. Troilite Isotope Fractionation Data Applied to Interpreting the Spheroid $\delta^{34}S$ Values

In this section the Canyon Diablo metallic spheroid $\delta^{34}S$ values are interpreted in light of the sulphur isotope fractionation results from the troilite, oxidation, evaporation and dissociation experiments.

It was previously pointed out (see Chapter 2, Section B) that if a Guassian distribution is assumed for the $\delta^{34}S$ values of the small spheroids then some of the small spheroids would have $\delta^{34}S$ values as great as about +6.3‰ and as low as about -5.5‰. However, the results of the troilite oxidation experiment place constraints on this range. In the troilite oxidation experiment the most negative $\delta^{34}S$ value (measured with respect to the starting material) observed was -0.79‰ for a sample that had experienced about 94% extent of reaction. Thus it is extremely unlikely that any of the small spheroids have $\delta^{34}S$ values that are more negative than about -0.8‰. It is also doubtful that any spheroids have $\delta^{34}S$ values that are even as negative as -0.8‰ since there is strongly suggestive evidence that the spheroids did not undergo extensive oxidation. This evidence is presented in Section D of this Chapter.

However, there seems to be a possibility that some of the spheroids have relatively large $\delta^{34}S$ values. The sulphur contents of individual spheroid cores reported by Blau, Axon and Goldstein (1973) range from 0.9 to 2.8 weight %. If it is assumed that all of the spheroids had an initial sulphur content of 2.8 weight % then the spheroid now having a sulphur content of 0.9 weight % has lost about 68% of its sulphur. If it is assumed that there was a uniform loss of sulphur from throughout the whole mass of the spheroid and that this loss occurred by dissociation/evaporation then Fig. 8 shows that the spheroid would have a $\delta^{34}S$ value of about 10‰. Thus it appears that there is a possibility that some of the small spheroids have a $\delta^{34}S$ value of about +6.3‰. Of course another possibility is that the spheroids may have differed from one another in sulphur content before either any oxidation or any dissociation/evaporation occurred.

It was also previously pointed out that the small spheroids have a mean $\delta^{34}S$ value that is significantly greater than the mean $\delta^{34}S$ value of either of the larger spheroid groups. This is most likely due to the small spheroids having a surface area to volume ratio greater than that of the larger spheroids so that a greater % of sulphur loss occurred in the small spheroids than occurred in the larger spheroids.

The sulphur isotope fractionation results from the troilite oxidation, evaporation and dissociation experiments are also useful in a discussion concerning the spheroid ablation experiment results. A plot of the sulphur contents and $\delta^{34}S$ values of the ablated spheroid samples from Tables 6, 7, 8 and 9 is shown in Fig. 9. Also included in the figure are two graphs of the extent of reaction versus $\delta^{34}S$ value equation [(6) on page 73] for the troilite two-branch dissociation/evaporation reaction.

Curve 1 is for a starting sulphur content of 0.8 weight percent, g equals 12.3, b equals 4.2 and P equals 0.1. Curve 2 is a similar graph except that the starting material has a sulphur content of 1.30 weight percent and g equals 13.5, b equals 5.4 and P equals 14.5. The layer samples from ablation series #2 were not plotted because it was not possible to correct their sulphur contents for the amount of lost layer material.

The sample with the most negative $\delta^{34}S$ value may not be significantly different from 0.0‰ since it is within two standard deviations of that value. This shows that probably

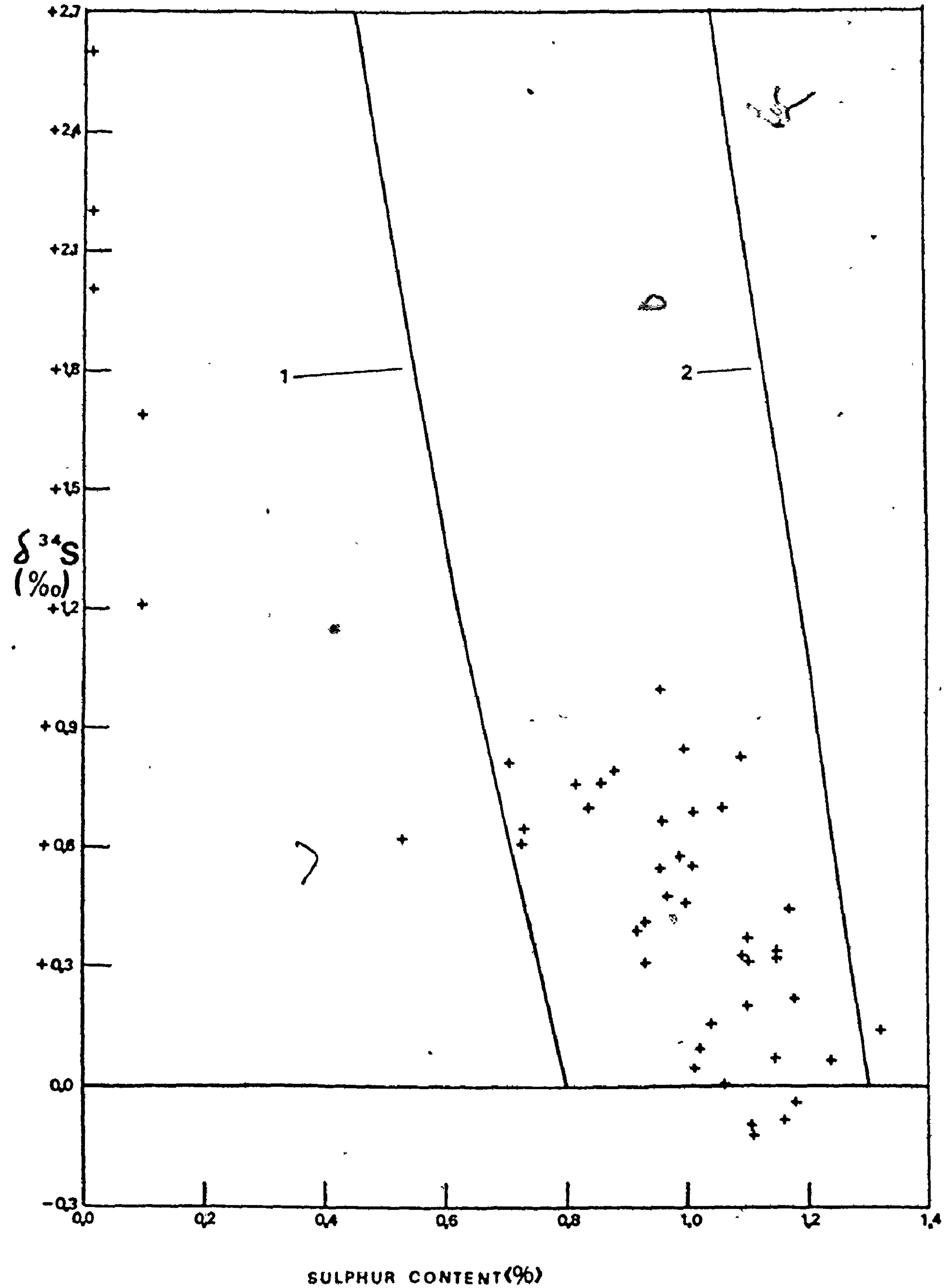

Figure 9. $\delta^{34}S$ Versus Sulphur Contents for the Ablated Spheroid Data

none of the samples experienced only oxidation as oxidation alone gives rise to residues with negative $\delta^{34}S$ values. It also means that almost all, if not all, of the samples have experienced a sulphur loss by evaporation/dissociation in a region having either low partial pressure of oxygen or near vacuum conditions.

If a sample point is found inside the region bounded by the curves it suggests that the samples may have started with a sulphur content in the range of 0.8 to 1.3 weight % and then lost sulphur by dissociation/evaporation. Only six of the forty-six experimental points lie significantly outside the curve-bound region and only one of those six is not a first-layer sample. The measured sulphur contents of the first-layer samples have doubtlessly been lowered by the presence of the silicate and oxides described earlier which occur only in the surface layers.

Some samples have approximately equal $\delta^{34}S$ values but unequal sulphur contents. Some of this sulphur content range may be due to oxidation of the spheroids that occurred in addition to the dissociation/evaporation. The oxidation could have reduced the sulphur content of a spheroid but only have changed the $\delta^{34}S$ value by the relatively small amount of about -0.33‰.

Some of the sulphur content range shown by the spheroid ablation samples may be due to the fact that during the course of a spheroid ablation process some spheroids lose more material than others so that the layer samples are a mixture of materials from slightly different depths and therefore different sulphur contents. The sulphur content range of the layer samples is probably more narrow than is apparent from Fig. 9 for the following reason. It was pointed out in Section C of Chapter 3 that some of the ablation material was lost during transfer to a weighing boat and that the lost material had a greater sulphur content than the material that was not lost. This means that the layer samples should have values for their sulphur contents that are greater than their present values. Such corrections would allow the curves to be drawn closer together.

However, it is not necessary to assume that the spheroids originally were all equal in sulphur content. Perhaps the spheroids were formed originally with different individual sulphur contents within the range 0.8 to 1.30 weight %. Later loss of sulphur by dissociation/evaporation would have produced the positive $\delta^{34}S$ values observed.

B. Nininger's Theory and Rinehart's Theory

One of the theories concerning the formation of the Canyon Diablo ~~m~~etallic spheroids is that of Nininger (1956) who reported Hawley's chemical analyses of spheroid samples (see page 40 in Chapter 3). Nininger observes that the spheroids are enriched in Ni and Co relative to the metallic area of the Canyon Diablo meteorite fragments. He explains this enrichment by suggesting that upon impact the meteoroid vaporized producing a metallic vapour cloud from which the spheroids having a wide range of chemical compositions would be produced by this mechanism. He explains the Ni and Co enrichment by suggesting that low-temperature oxidation taking place over tens of thousands of years would allow to survive only those spheroids with certain erosion-resistant compositions.

One objection to this theory is that Mead et al. (1965) found what they believe to be relict schreibersite grains in the spheroids that had not been completely melted but were transferred largely intact from the meteoroid to the spheroids.

Another objection is concerned with the distribution of the spheroids in the crater area. The following description of the type and distribution of meteoritic debris in the neighbourhood of the crater is essentially the same as that of Blau, Axon and Goldstein (1973). Nininger (1956) and Rinehart (1958) both found that the metallic spheroids are concentrated in ray-like throw-out patterns extending from the crater. They are accompanied by a much smaller proportion of "sluglets" having masses similar to the metallic spheroids but with a structure and chemical composition identical to the larger Canyon Diablo meteorite fragments. Also, there are similarly-sized iron-oxide and magnetite particles but these too are a small percentage of the total particle and spheroid mass. The ray systems for the metallic spheroids and the other particles concentrate predominantly in the N.E. quarter and extend more than three km onto the surrounding plains. The heavily shocked but unmelted fragments of ounce to pound weight that have come to be known as "rim" specimens are found in the same approximate directions but are chiefly located just beyond the crater rim. The "plains" specimens are farther from the crater and more uniformly distributed around the crater than are the "rim" specimens. The "rim" and "plains" Canyon Diablo meteorite fragments total about 25 tons while the metallic spheroids and other particles have a mass of about 10,000 to 12,000 tons.

Rinehart (1958) suggests that the very close similarity between the distribution of ponderable chunks and the smaller spheroids is strong evidence that the spheroids were ejected in the liquid state. Nininger's vapour cloud theory would lead to a circularly symmetrical pattern centered on the crater rather than the observed distribution. Nininger has suggested that the spheroids may have been blown by wind to their present position but Rinehart found no evidence of winnowing (sorting by weight). Rinehart suggests that the vapour would be oxidized and drift off as a fine powder. Rinehart has also suggested that selective weathering explains the enrichment of Ni and Co in the spheroids. A major objection to this idea is that the sheroids are coated with a silicate and oxide layer (Mead et al., 1965) so that they all would be about equally resistant to weathering.

Nininger's theory, however, does allow for vacuum dissociation/evaporation since the spheroids are postulated to solidify in an oxygen-free atmosphere. However, it is not the only possibility for a vacuum region occurring at the time of the impact. Vand (1965) describes the air flow and shock wave system formed near a spherical meteoroid during its supersonic passage through the atmosphere at 30 km/sec. He points out that a conical region of near-vacuum pressures forms directly behind the meteoroid. Also, calculations were carried out that show that the density of air in the hot train produced by the meteoroid's passage is only 0.03 atmosphere and that faster meteoroids would give rise to pressures less than 0.03 atmosphere.

C. The Theory of Blau, Axon and Goldstein

Blau, Axon and Goldstein (1973) used a microprobe to do a bulk chemical analysis on the oxide-free cores of 14 Canyon Diablo metallic spheroids having diameters in the range 0.7 - 1.8 mm. They found average values of 16.1 weight percent Ni, 0.9 weight percent Co, 1.6 weight percent S and 1.0 weight percent P. They also provide values of 7.3 weight percent Ni, 0.45 weight percent Co, 0.008 weight percent S and 0.19 weight percent P for the metallic (inclusion-free) area of the Canyon Diablo meteorite. They point out that the spheroid cores are enriched in Ni, Co, S and P compared to the metallic area of the Canyon Diablo fragments.

They also state that troilite (FeS) nodules are generally associated with schreibersite, $(Fe, Ni)_3P$, inclusions in the Canyon Diablo meteorite fragments and that troilite-metal interfaces are the easiest to melt by shock processes. Thus a possible production of a sulfide-metal-phosphide liquid by shock provides a mechanism for the enrichment of the spheroids in Ni, S and P. The more heavily shocked material (liquid or vapour) would reach higher effective temperatures and be thrown farther from the crater.

Since schreibersite and troilite are Co-poor relative to the metallic area of the meteorite, this mechanism would produce spheroids depleted in Co rather than enriched. They explain the observed enrichment by stating that the spheroids are oxidized as they travel from the impact site through the air. They state that Fe, P and S will be preferentially oxidized with respect to Ni and Co so that Ni and Co are enriched and the others depleted. The amount of oxidation regulates the final composition of the spheroid.

Kelly, Holdsworth and Moore (1974), however, point out that once the shock-produced liquid is formed, the Ni/Co ratio is fixed and will not change with oxidation. Blau's mechanism should produce particles with a Ni/Co ratio much higher than that of the bulk meteorite. Both Blau's and Kelly's data show that this is not the case. An objection presented in this thesis to Blau's theory is that the spheroids may in fact <u>not</u> be enriched in sulphur and phosphorous relative to the bulk meteoroid as they imply. Sulphur in iron meteorites exists primarily in the form of troilite (FeS) nodules that are very irregularly distributed throughout the nickel-iron matrix (Mason, 1962). These inclusions are frequently 1 cm or more in diameter although occasionally huge nodules of troilite from 10 to 15 cm in diameter are observed (Goldberg, Uchiyama and Brown, 1951). The usual procedure used in the chemical analysis of an iron meteorite is to avoid the inclusions and work only with a sample of the nickel-iron matrix so that these analyses are unsuitable for the calculation of the sulphur content of the meteorite as a whole (Henderson and Perry, 1958).

Two attempts have been made to determine the amount of troilite in the Canyon Diablo meteorite. Moore, Birrell and Lewis (1967) made a modal (point count) analysis of a number of sections of different specimens using a reflected light microscope equipped with a mechanical stage to move the specimen. The phase present under the crosshairs was recorded for each movement of the stage. Using this technique they obtained a value of 0.91 area percent troilite. However, Moore (private communication) considers that the following value obtained by Henderson and Perry is more nearly correct.

Henderson and Perry (1958) measured the width across a section and then measured the total distance occupied by troilite along that line. Similar parallel traverses were made at one-eighth inch intervals. Using this technique a value of 5.95 area percent troilite was obtained.

However, they point out that only a small number of sections were measured whereas tons of the Canyon Diablo meteorite have been recovered so that the areas that were measured were too small to represent the meteorite as a whole.

The density of the Canyon Diablo meteorite as a whole is 7.83 gm/cc (Moore, Birrell and Lewis, 1967) and the density of troilite is 4.74 gm/cc (Weast, 1968). Using these density values, 0.91 area percent troilite corresponds to 0.2 weight percent sulphur and 5.95 area percent troilite corresponds to 1.32 weight percent sulphur.

Moore, Lewis and Nava (1969) found a value of 0.002 weight percent sulphur by chemical analysis for the inclusion-free matrix of the Canyon Diablo meteorite so that it is apparent that the sulphur does in fact exist primarily in the form of troilite nodules and the above values need not be corrected for the sulphur content of the matrix.

It is apparent from the above information that the spheroids may <u>not</u> be enriched in sulphur compared to the bulk meteoroid. The value of 1.32 weight percent is not much different from the 1.6 weight percent value found by Blau, Axon and Goldstein for their spheroid cores.

A similar situation may exist for phosphorous. C. B. Moore in Mason (1971) states that the P content of iron meteorites is usually underestimated because large schreibersite, $(Fe,Ni)_3P$, inclusions are avoided in sampling for chemical analysis. Moore reports that four out of eleven iron meteorite P analyses, performed by point counting techniques, yielded values in the range 1.0 to 1.3 weight percent. Unfortunately the Canyon Diablo meteorite was not analysed in a similar manner by the same authors. However, it is certainly possible that the Canyon Diablo meteoroid contained 1.0% by weight P which is the value Blau, Axon and Goldstein found for the spheroids. It is suggested in this thesis that the sulphur and phosphorous contents of the spheroids could possibly be explained by just having the meteorite homogenized upon impact. Homogenization of the meteoroid is a part of the theory of Kelly, Holdsworth and Moore (1974) which is described below.

D. The Theory of Kelly, Holdsworth and Moore

Kelly, Holdsworth and Moore (1974) performed atomic absorption analyses on the oxide-free cores of 25 Canyon Diablo metallic spheroids for Fe, Ni, Co and Cu. They normalized to 100% both this data and the data for the bulk meteorite so that comparison could be made. They found that Ni, Co and Cu were enriched to the same degree by factors from 2 to 3 compared to the bulk meteorite. Plots of Co and Cu versus Ni show that both are positively correlated with Ni and the regression lines pass close to the bulk meteorite composition.

To explain these results the authors suggest that a portion of the meteoroid was melted and homogenized by the impact. The spheroids were formed from this liquid and were then oxidized as they travelled through the air. The Fe was oxidized preferentially to Ni, Co and Cu so that the spheroids became enriched in the latter elements.

Fig. 7 in their paper shows that from $\sim$55% to $\sim$65% of the initial Fe in the spheroids must have been removed by oxidation in order to produce the observed Ni enrichment. Kelly, Holdsworth and Moore (1974), and Blau, Axon and Goldstein (1973) state that both S and P are more readily oxidized than is Fe. Kelly, Holdsworth and Moore neglect to make the conclusion that if $\sim$60% of the Fe is removed then even more S and P would also be removed. This means that the Canyon Diablo meteoroid must have had at least $^{100}/40$ times the S and P found in the present day spheroids. Blau, Axon and Goldstein (1973) provide mean weight percent values of S and P contents for the spheroids of 1.61 and 1.0 respectively so that the Canyon Diablo meteoroid must have had values greater than those, the factor depending on the oxidation rate ratios of P and S relative to Fe.

It is unfortunate that Kelly, Holdsworth and Moore did not also measure the sulphur content of the spheroids.

If their theory was correct it might be expected that a negative correlation would be found between the Ni contents and S (or P) contents since the Ni enrichment is supposed to be due to oxidation. Plots of percent S and percent P versus percent Ni using the data of Blau, Axon and Goldstein are shown in Figs. 10 and 11 respectively. It is apparent that no such negative correlations exist. This implies that oxidation did not produce the observed Ni and Co enrichment.

E. Homogeneity of the Meteoroid

It is suggested here that the spheroids were formed from a large portion of the meteoroid having more Ni and Co than the portion from which the Canyon Diablo meteorite fragments were derived. There is some evidence of inhomogeneity in the Canyon Diablo meteoroid.

Less than twelve Canyon Diablo specimens are classified as medium octahedrites, whereas all of the thousands of other Canyon Diablo specimens are classified as coarse octahedrites (Lipschutz, 1965). These anomalous individuals contain 8.09 weight percent nickel and have palladium concentrations of 5.30 ppm in contrast to 7.11 weight percent nickel and 3.98 ppm palladium for the vast majority (Heymann, 1964). However, Lipschutz (1965) concluded from

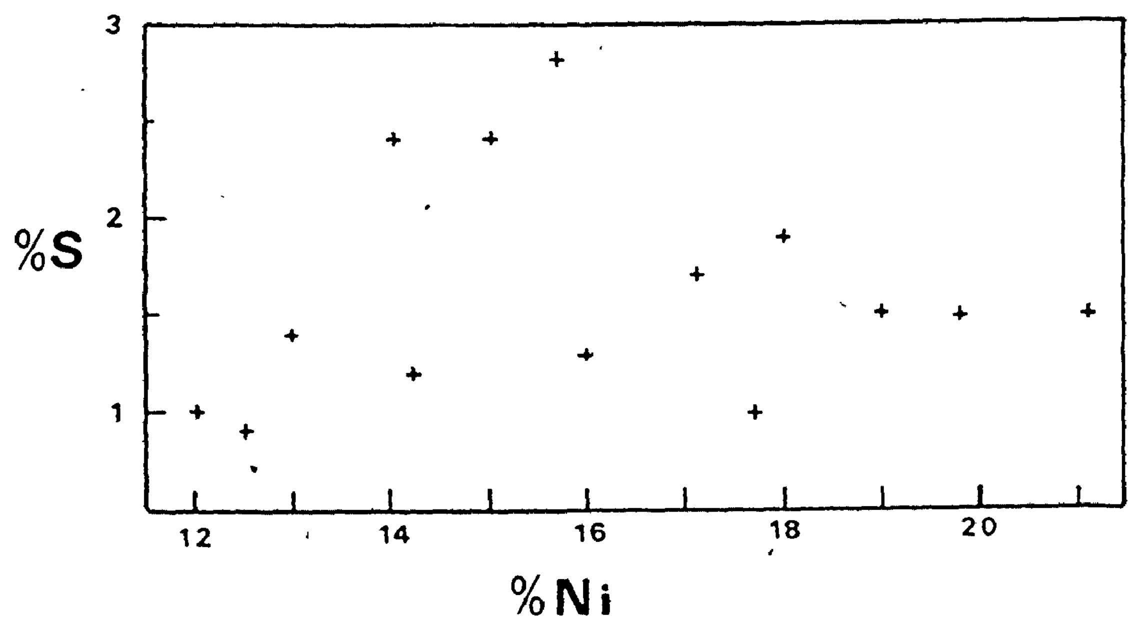

Figure 10. % S Versus % Ni for Individual Spheroid Cores from the Data of Blau et al. (1973)

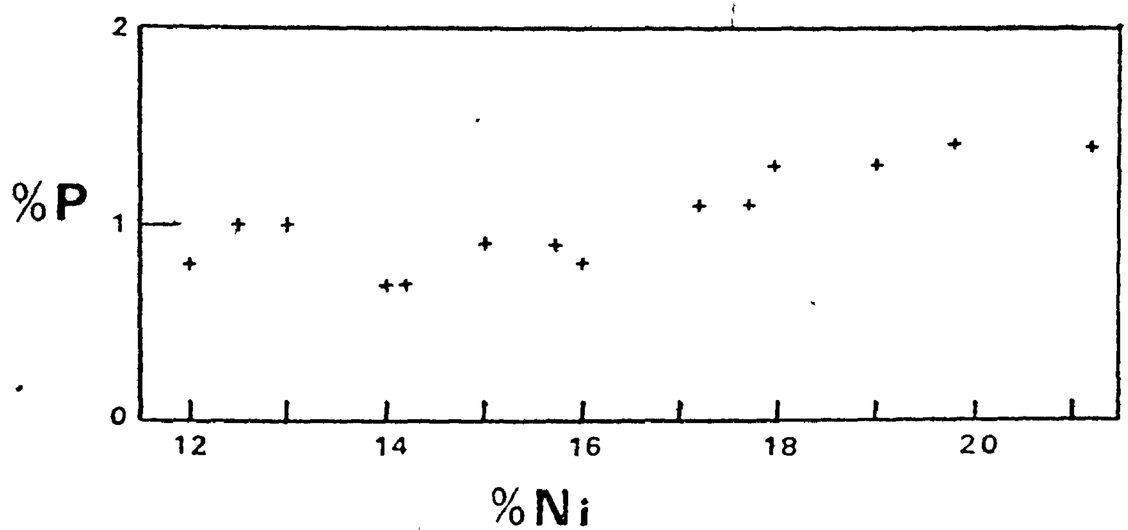

Figure 11. % P Versus % Ni for Individual Spheroid Cores from the Data of Blau *et al.*, (1973)

his shock effect evidence and Heymann's cosmogenic rare gas evidence that these anomalous individuals and the thousands of others all were fragments of the one meteoroid rather than being fragments from two separate meteoroids. Lipschutz, therefore, further concluded that substantial structural and compositional variations may exist within an individual meteoroid.

The anomalous specimens, together with other normal specimens, were found on the crater rim. This, and other observations, led Nininger (1950) to suggest that the specimens found on or near the crater rim differ from the specimens found on the plains surrounding the crater. Moore, Birrell and Lewis (1967) studied these differences in detail and found that some of these differences were statistically significant. They found significantly more nickel in the rim specimens than in the plains specimens and the rim specimens were found to have been shocked to a greater degree than had been the plains specimens. Also, the rim specimens were found to have a greater weight density than that of the plains specimens. Moore, Birrell and Lewis concluded that there was in fact inhomogeneity in the Canyon Diablo meteoroid but whether or not it possessed sharp boundaries or was more of a transitional nature was difficult to assess.

F. Break-up of the Meteoroid

There is also evidence that the Canyon Diablo fragments are not samples from the meteoroid as a whole but rather were derived from only the outermost portions of it. Heymann et al. (1965) studied the cosmogenic rare gas contents and shock indicators of fifty-six Canyon Diablo fragments. They concurred with the shock findings of Moore, Birrell and Lewis (1967) and also concluded that all but ten of the samples came from a depth of less than 1.8 m from the surface of the pre-atmospheric meteoroid. The rim specimens came from a mean depth of 121 cm and the plains specimens came from a mean depth of 81 cm. They stated that their findings therefore support Öpiks (1958) conclusion that the surviving Canyon Diablo fragments came from the rear surface of the meteoroid.

Estimates of the Canyon Diablo meteoroid vary from 10,000 tons (Rinehart, 1958) to 5,000,000 tons (Rostoker, 1953). Bjork (1961) provides a narrower range, 30,000 tons to 194,000 tons, corresponding to impact velocities of 72 km/sec or 11 km/sec respectively. If the average meteorite velocity of 30 km/sec is assumed then the corresponding mass is 72,000 tons. Shoemaker (1963) provides a mass estimate of 63,000 tons but has since revised that to 150,000 tons (Shoemaker, private communication, 1976). The diameter of a spherical mass of 63,000 tons having a density of 7.85 gm/cc is 24.8 m and that of a spherical mass of 150,000 tons is 33.1 m. It is evident that the Canyon Diablo meteorite fragments are in fact derived from the outermost portions of the meteoroid.

Blau, Axon and Goldstein (1973) have summarized the steps in the production and dispersion of the Canyon Diablo meteoritic debris. They suggest that the plains specimens were cracked or spalled off the meteoroid when it encountered the denser layers of Earth's atmosphere. They quote reports of heat-altered zones on some of the specimens where the removal by terrestrial corrosion had been small. This evidence is supportive of these specimens having an independent ablative flight through the atmosphere. This atmospheric break-up theory also explains why the plains specimens have received less shock than the rim specimens even though the former are found farther from the crater than the latter.

When the meteoroid encountered the surface of the earth shock pressures of increasing magnitude began to pass back through the meteoroid. When the lower pressure waves reached the free surfaces of the meteoroid body they were internally reflected to produce a rarefaction wave which spalled off the rim specimens. The momentum trapped in the fragment carried it to its present position. These rim specimens were from deeper in the meteoroid than were the plains specimens. It was also previously noted that the rim specimens contain more nickel than the plains specimens.

Olshaker and Bjork (1961) state that shocked material is first compressed adiabatically by a shock during which time its entropy is increased and then in return to low pressure the adiabatic expansion takes place isentropically leaving the material in a heated state. Shocks of low strength will leave the material in the solid state, but heated to some degree. Stronger and stronger shocks lead to fusion, heated liquid, vaporization and superheated vapor as the final state.

Blau, Axon and Goldstein state that the more heavily shocked material would reach higher effective temperatures and would be thrown farther from the crater than the rim specimens. As mentioned before, they suggest that the troilite-schreibersite regions would be easier melted than the other regions and suggest that the spheroids were formed from this selectively-melted liquid. They further envision the remaining meteoroid portion to have vaporized.

Kelly, Holdsworth and Moore have criticized the selective melting hypothesis by stating that the rise in pressure is too sharp to allow it to occur. In general, however, the description of the impact events is consistent with shock events as described by Olshaker and Bjork (1961).

As the rarefraction wave passed back through the meteoroid it encountered material under increasing pressures. In this manner, the deeper material is heated to a greater temperature than the shallower material.

It is suggested by this author that the deeper portions of the meteoroid had a greater nickel content than the outer portions. It is further suggested that the spheroids were formed from this nickel-rich material. They then experienced the near-vacuum of the meteoroid train during which time they lost a relatively small amount of sulphur by evaporation/dissociation. After this they may also have experienced oxidation as they left the low-pressure zone and travelled through the atmosphere. The spheroids were than encased in a skin of silicate which sealed them off from the atmosphere. Mead et al. (1965) suggest that the siliceous glass coating on the spheroids indicates that they must have consolidated and cooled in an environment where a great deal of silicate vapor was also condensing. They also suggest that the angular fragments in the glass probably came from the sandstone found in the crater area that was pulverized by the impact. No one has suggested an origin for the silicate vapor.

G. Summary

The sulphur contents and $\delta^{34}S$ values of a number of Canyon Diablo metallic spheroid samples of three different sizes were measured. It was found that the spheroids are slightly enriched in the heavier sulphur isotopes relative to the troilite from the Canyon Diablo meteorite fragments, having mean $\delta^{34}S$ values of +0.23‰ and +0.40‰ for the large and small spheroids respectively.

Ablations were performed on six different spheroid samples of two different sizes in order to investigate the variation of $\delta^{34}S$ values and sulphur contents with depth within the spheroids. It was found that the outermost layer samples have $\delta^{34}S$ values in the range from +1.22‰ to +2.60‰. The material inside the outermost layer was found to have smaller but still positive $\delta^{34}S$ values. It was also found that the inner material had a greater sulphur content than did the outer material.

The sulphur isotope effect associated with the oxidation of troilite at ∿1200°C was measured. It was found that the residue is slightly depleted in the heavier isotopes and the SO_2 is slightly enriched. No regular relationship was found between the extent of reaction and the $\delta^{34}S$ values (relative to the starting material) of the SO_2 samples and the residue samples. The mean of the $\delta^{34}S$ values of the residue samples was found to be -0.33‰.

The sulphur isotope effects associated with the dissociation and evaporation of troilite at $\sim$1200°C were measured. It was found that evaporation and dissociation occurred simultaneously in a two-branch reaction. It was assumed that the dissociation and evaporation were first-order reactions and it was found that the $\delta^{34}S$ values (relative to the starting material) of the components and the extent of reaction data were consistent with the predictions of these equations. It was found that the sulphur isotope effects associated with the evaporation and dissociation of troilite were (+4.8 $\pm$ 0.3)‰ and (+12.9 $\pm$ 0.3)‰ respectively where the products were enriched in lighter isotopes. These results have already proved useful elsewhere in the interpretation of the $\delta^{34}S$ values and sulphur contents in the lunar material (Thode and Rees, 1976).

A review of the theories of other authors concerning the formation of the Canyon Diablo metallic spheroids was carried out and a discussion of the evidence for and against each theory was presented. A new theory was presented which suggests that an inner portion of the meteoroid had greater Ni and Co contents than the outermost portions from which the Canyon Diablo meteorite fragments were derived. It was suggested that this portion of the meteoroid was shock-melted and dispersed to become the spheroids. The $\delta^{34}S$ values of the spheroids became positive due to loss of sulphur by dissociation and evaporation in the near-vacuum environment of the meteoroid train.

APPENDIX I

WEIGHT OF THE MEDIUM AND LARGE SPHEROIDS

TABLE 26

WEIGHT OF THE MEDIUM SPHEROIDS

Sample number	Number of spheroids	Weight (grams)	Mean weight (milligrams)
30	30	0.13310	4.437
31	28	0.12723	4.544
32	23	0.11637	5.060
33	22	0.12372	5.624
34	23	0.11899	5.173
35	30	0.11843	3.948
36	23	0.10904	4.741
37	22	0.10931	4.969
38	25	0.11292	4.517
39	24	0.10680	4.450
40	23	0.11214	4.876
41	26	0.11531	4.435
57	24	0.11025	4.594
58	24	0.10932	4.555
61	27	0.11146	4.128
62	23	0.11159	4.852
63	23	0.11109	4.830
64	25	0.11107	4.443
65	23	0.10900	4.739
66	28	0.11101	3.965
Ablation #4	200	0.73717	3.686
Ablation #5	200	0.75425	3.771
Ablation #6	200	0.73940	3.697
Sum	1096	4.51897	-----

Mean weight = 4.12 mg

TABLE 27

WEIGHT OF THE LARGE SPHEROIDS

Sample number	Number of spheroids	Weight (grams)	Mean weight (milligrams)
43	21	0.11560	5.505
44	23	0.11619	5.052
45	22	0.11531	5.241
46	22	0.11071	5.032
47	21	0.11010	5.243
48	21	0.10895	5.188
50	22	0.11071	5.032
51	25	0.11250	4.500
52	20	0.10187	5.094
54	24	0.11373	4.738
55	20	0.10951	5.476
56	24	0.11052	4.605
Ablation #1	200	0.99179	4.959
Ablation #2	200	0.97058	4.853
Ablation #3	200	0.95185	4.759
Sum	865	4.24992	-----

Mean weight = 4.91 mg

APPENDIX II

$\delta^{34}S$ (‰) VALUES AND SULPHUR CONTENTS FOR THE WHOLE SPHEROIDS

TABLE 28

SULPHUR CONTENT AND $\delta^{34}S$ VALUES FOR THE SMALL SPHEROIDS

Weight of spheroid sample (grams)	Weight of Ag_2S (mg)	Weight % sulphur	$\delta^{34}S$ (‰)
0.10127	6.08	0.777	+0.39
0.12966	8.39	0.837	+0.28
0.12927	8.45	0.846	+0.59
0.12940	8.43	0.843	+0.14
0.12966	8.16	0.814	+0.34
0.12955	8.30	0.829	+0.50
0.12921	9.20	0.921	+0.29
0.12943	8.19	0.819	+0.74
0.12940	8.53	0.853	+0.49
0.12962	8.05	0.804	+0.61
0.12905	7.76	0.778	+0.30
0.12937	7.31	0.731	+0.26
0.12976	8.60	0.858	+0.31
0.13010	8.40	0.835	+0.36

TABLE 29

SULPHUR CONTENT AND $\delta^{34}S$ VALUES FOR MEDIUM SPHEROIDS

Weight of spheroid sample (grams)	Weight of Ag_2S (mg)	Weight % sulphur	$\delta^{34}S$ (‰)
0.13310	10.70	1.040	+0.04
0.12723	8.46	0.860	+0.22
0.11637	8.24	0.916	+0.05
0.12372	8.75	0.915	+0.20
0.11899	9.28	1.009	+0.53
0.11843	8.88	0.970	+0.14
0.10904	8.34	0.990	+0.10
0.10931	8.35	0.988	+0.34
0.11214	8.14	0.939	+0.45
0.11531	9.10	1.021	+0.19
0.11025	9.10	1.068	+0.10
0.11146	9.46	1.102	+0.28
0.11159	8.82	1.023	+0.28
0.11109	8.30	0.967	+0.40
0.11107	9.41	1.096	+0.04
0.10900	9.20	1.092	+0.23
0.11101	9.33	1.087	+0.25

TABLE 30

SULPHUR CONTENT AND $\delta^{34}S$ VALUES FOR THE LARGE SPHEROIDS

Weight of spheroid sample (grams)	Weight of Ag_2S (mg)	Weight % sulphur	$\delta^{34}S$ (‰)
0.11560	8.34	0.934	+0.12
0.11619	9.36	1.042	+0.23
0.11531	8.13	0.912	+0.13
0.11071	8.23	0.962	+0.13
0.11010	8.40	0.987	+0.20
0.10895	8.54	1.014	+0.05
0.10956	8.00	0.945	+0.18
0.11071	8.43	0.985	+0.28
0.11250	8.44	0.971	+0.50
0.10187	6.76	0.859	+0.24
0.11373	8.93	1.016	+0.11
0.10951	8.96	1.059	+0.49
0.11052	8.85	1.036	+0.16

APPENDIX III

SPHEROID ABLATION DATA

TABLE 31

THE LAYER SAMPLE DATA

Series number, Ablation number	Weight before ablation (grams)	Weight material collected (grams)	Weight material lost (grams)	Weight Ag_2S (mg)	$\delta^{34}S$ (‰)
1,1	0.99179	0.13937	0.07070	[3]0.89	+2.20
1,2	0.78172	0.09172	0.01888	[3]----	[3]-----
1,3	0.67112	0.08043	0.00956	2.91	+0.60
1,4	0.58113	0.05950	0.02008	2.58	+0.62
1,5	0.50155	0.05695	0.02765	2.16	+0.64
2,1	0.97058	0.13548	[2]-------	0.37	+2.61
2,2	[2]-------	0.09089	[2]-------	4.97	+0.84
2,3	[2]-------	0.07327	[2]-------	3.30	+0.40
2,4	[2]-------	0.05504	[2]-------	2.69	+0.08
2,5	[2]-------	0.04091	[2]-------	1.80	+0.15
3,1	0.95185	0.12223	0.08045	0.60	+2.04
3,2	0.74911	0.08138	0.02809	4.04	+0.76
3,3	0.63970	0.07213	0.02128	3.79	+0.79
3,4	0.54629	0.05380	0.01634	2.60	+0.76
3,5	0.47615	0.04602	0.01382	1.99	+0.61

continued ...

TABLE 31

(continued)

THE LAYER SAMPLE DATA

Series number, Ablation number	Weight before ablation (grams)	Weight material collected (grams)	Weight material lost (grams)	Weight Ag_2S (mg)	$\delta^{34}S$ (‰)
4,1	0.73717	0.09830	0.06085	[1]-----	[1]-----
4,2	0.57802	0.05882	0.02498	[1]-----	[1]-----
4,3	0.49422	0.04470	0.02492	2.41	+0.84
4,4	0.42460	0.03977	0.01963	2.05	+0.85
4,5	0.36520	0.03209	0.01513	1.60	+0.67
5,1	0.75425	0.09279	0.08062	0.41	+1.66
5,2	0.58084	0.06286	0.03132	3.17	+1.02
5,3	0.48666	0.05154	0.02004	2.90	+0.57
5,4	0.41508	0.04054	0.01949	2.04	[1]-----
5,5	0.35505	0.02693	[4]0.01882	1.38	+0.04
6,1	0.73940	0.08760	0.06521	0.40	+1.22
6,2	0.58659	0.06225	0.02956	3.47	+0.71
6,3	0.49478	0.04774	0.02352	2.75	+0.31
6,4	0.42352	0.03315	0.02618	1.84	[1]-----
6,5	0.36419	0.03836	0.09403	1.76	+0.72

[1]Sample lost.

[2]Not recorded.

[3]The material from the first two ablations was mixed together.

[4]Ablation period of 5 hours and 26 minutes.

TABLE 32

ABLATED SPHEROID DATA

Series number, [4]Size	Spheroid number	Spheroid weight (grams)	Spheroid mean weight (mg)	Weight Ag_2S (mg)	$\delta^{34}S$ (‰)
1,L	[2]50	0.12494	2.50	[1]-----	[1]----
1,2L	[2]50	0.12510	2.50	[1]-----	[1]----
1,3L	[2]50	0.11949	2.39	10.74	-0.09
1,4L	[2]49	0.04638	0.95	3.61	+0.04
1,F	--	0.02509	----	1.94	+0.45
2,L	40	0.15197	3.80	13.04	-0.12
2,2L	45	0.09949	2.21	8.66	-0.08
2,3L	50	0.08322	1.66	6.81	0.00
2,4L	65	0.06079	0.94	4.81	+0.11
2,F	--	0.02359	----	1.99	+0.69
3,L	30	0.11890	3.96	10.77	-0.10
3,2L	40	0.10465	2.62	9.51	-0.04
3,3L	60	0.10030	1.67	8.51	+0.36
3,4L	70	0.05860	0.84	4.47	+0.58
3,F	--	0.03386	----	2.42	+0.41
4,L	25	0.07663	3.07	6.98	+0.21
4,2L	35	0.07066	2.02	7.14	+0.15
4,3L	50	0.07582	1.52	6.76	+0.33
4,4L	90	0.07288	0.81	6.18	+0.20
4,F	--	0.02146	----	1.61	+0.47

continued ...

TABLE 32
(continued)

ABLATED SPHEROID DATA

Series number, [4]Size	Spheroid number	Spheroid weight (grams)	Spheroid mean weight (mg)	Weight Ag_2S (mg)	$\delta^{34}S$ (‰)
5,L	25	0.07908	3.16	7.60	+0.06
5,2L	35	0.07367	2.10	6.54	+0.07
5,3L	50	0.07082	1.42	5.97	+0.32
5,4L	90	0.06312	0.70	5.08	+0.16
5,F	--	0.02312	----	1.64	+0.38
6,L	25	0.06358	2.54	5.77	+0.46
6,2L	35	0.05880	1.68	[3]4.41	[1]-----
6,3L	50	0.05677	1.14	5.04	+0.32
6,4L	90	0.04074	0.45	3.01	+0.55
6,F	--	0.01198	----	0.86	+0.31

[1]Sample lost.

[2]Spheroids not size separated by eye.

[3]Possible loss of Ag_2S due to the shattering of the centrifuge tube.

[4]L represents largest, 2L represents second largest, etc.; F represents fragments.

BIBLIOGRAPHY

Beaver, E. M., An Automatic Ratio Readout System for a Double Collection Mass Spectrometer, Mass Spectrometry 21, No. 1, 37-44 (1973).

Bigeleisen, J. and Wolfsberg, M., Theoretical and Experimental Aspects of Isotope Effects in Chemical Kinetics, Advan. Chem. Phys. 1, 16 (1958).

Bjork, R. L., Analysis of the Formation of Meteor Crater, Arizona: A Preliminary Report, J. Geophys. Res. 66, 10, 3379-3387 (1961).

Blau, P. J., Axon, H. J. and Goldstein, J. I., Investigation of the Canyon Diablo Metallic Spheroids and Their Relationship to the Breakup of the Canyon Diablo Meteorite, J. Geophys. Res. 78, 2, 363-374 (1973).

Chang, S., Lennon, K. and Gibson, E. K., Abundances of C, N, H, He, and S in Apollo 17 Soils from Stations 3 and 4: Implications for Solar Wind Exposure Ages and Regolith Evolution, Proc. Fifth Lunar Sci. Conf., Suppl. 5, Vol. 2, Geochim. Cosmochim. Acta, 1785-1800 (1974).

Chao, E. C. T., Dwornik, E. J. and Littler, J., New Data on the Nickel-Iron Spherules from Southeast Asian Tektites and Their Implications, Geochim. Cosmochim. Acta 28, 971-980 (1964).

Chao, E. C. T., Impact Cratering Models and Their Application to Lunar Studies - a Geologist's View, Proc. Fifth Lunar Sci. Conf., Geochim. Cosmochim. Acta, Suppl. 5, Vol. 1, 35-52 (1974).

Chapman, C. R., The Nature of Asteroids, Scientific American 232, 1, 24-33 (1975).

Charters, A. C., High-Speed Impact, Scientific American 203, 4, 128-140 (1960).

Clayton, R. N. and Mayeda, T. K., The Use of Bromine Pentafluoride in the Extraction of Oxygen From Oxides and Silicates for Isotopic Analysis, Geochim. Cosmochim. Acta 27, p. 43 (1963).

Dence, M. R., Impact Melts, J. Geophys. Res. 71, 23, 5552-5574 (1971).

Gibson, E. K., Chang, S., Lennon, K., Moore, G. W. and Pearce, G. W., Sulfur Abundances and Distributions in Mare Basalts and Their Source Magmas, Proc. Sixth Lunar Sci. Conf., Suppl. 6, Vol. 2, Geochim. Cosmochim. Acta, 1287-1301 (1975).

Goldberg, E., Uchiyama, A. and Brown, H., The Distribution of Nickel, Cobalt, Gallium, Palladium and Gold in Iron Meteorites, Geochim. Cosmochim. Acta 2, 1-25 (1951).

Goldstein, J. I. and Yakowitz, H., Metallic Inclusions and Metal Particles in the Apollo 12 Lunar Soil, Proc. Second Lunar Sci. Conf., Geochim. Cosmochim. Acta, Vol. 1, 177-191 (1971).

Harrison, A. G. and Thode, H. G., The Kinetic Isotope Effect in the Chemical Reduction of Sulphate, Trans. Faraday Soc. 53, No. 420, 1648-1651 (1957).

Hartmann, W. K., The Smaller Bodies of the Solar System, Scientific American 233, 3, 143-159 (1975).

Henderson, E. P. and Perry, S. H., Studies of Seven Siderites, Proc. U. S. Nat. Mus. 107, 339-403 (1958).

Heymann, D., Origin of the Canyon Diablo No. 2 and No. 3 Meteorites, Nature 204, 819-820 (1964.

Heymann, D., Lipschutz, M. E., Nielson, B. and Anders, E., Canyon Diablo Meteorite: Metallographic and Mass Spectrometric Study of 56 Fragments, J. Geophys. Res. 70, 215-224 (1965).

Hulston, J. R., Variations in the Ratios of the Four Stable Sulphur Isotopes in Meteorites and Their Relation to Chenical and Nuclear Effects, Ph.D. Thesis, McMaster University (1964).

Hulston, J. R. and Thode, H. G., Variations in the ^{33}S, ^{34}S and ^{36}S Contents of Meteorites and Their Relation to Chemical and Nuclear Effects, J. Geophys. Res. 70, No. 14, 3475-3484 (1965).

Hultgren, R., Orr, R. L., Anderson, P. D. and Kelly, K. K., Selected Values of Thermodynamic Properties of Metals and Alloys, 963 pp., Wiley, (1963). (Quoted in Kelly et al., 1974).

Kelly, W. A., Holdsworth, E. and Moore, C. B., The Chemical Composition of Metallic Spheroids and Metallic Particles Within Impactite from Barringer Meteorite Crater, Arizona, Geochim. Cosmochim. Acta 38, 533-543 (1974).

Kerridge, J. F., Kaplan, I. R. and Petrowski, C., Evidence for Meteoritic Sulfur in the Lunar Regolith, Proc. Sixth Lunar Sci. Conf., Suppl. 6, Vol. 2, Geochim. Cosmochi. Acta, 2151-2162 (1975).

Kinslow, R., Collisions at High Velocity, Intern. Sci. Technol. 38-47, April (1965).

Lewis, J. S., A Possible Origin for Sulphates and Sulphur in Meteorites, Earth Planet. Sci. Letts. 2, 29-32 (1967).

Lewis, J. S. and Krouse, H. R., Isotopic Composition of Sulphur and Sulphate Produced by Oxidation of FeS, Earth Planet. Sci. Letts. 5, 425-428 (1969).

Lipschutz, M. E., Origin of Atypical Meteorites from the Arizona Meteorite Crater, Nature 208, 636-638 (1965).

Lord Rayleigh (Strutt, R. J.), Theoretical Considerations Respecting the Separation of Gases by Diffusion and Similar Processes, Phil. Mag., 42, 493-498 (1896).

Luke, C. L., Determination of Total Sulphur in Rubber, Industrial and Engineering Chemistry 15, No. 9, 602-604 (1943).

Lusk, J. and Crocket, J. H., Sulphur Isotope Fractionation in Coexisting Sulfides from the Heath Steele B-1 Orebody, New Brunswick, Canada, Econ. Geol. 64, 147-155 (1969).

Macnamara, J. and Thode, H. G., Comparison of Isotopic Constitution of Terrestrial and Meteoritic Sulphur, Phys. Rev. 78, 307-308 (1950).

Mason, B., Meteorites, John Wiley and Sons, (1962).

Mason, B., (ed.), Handbook of Elemental Abundances in Meteorites, Gordon and Breach Science Publishers, New York (1971).

Mead, C. W., Littler, J. and Chao, E. C. F., Metallic Spheroids from Meteor Crater, Arizona, Amer. Mineral. 50, 667-681 (1965).

Monster, J., Anders, E. and Thode, H. G., $^{34}S/^{32}S$ Ratios for the Different Forms of Sulphur in the Orgueil Meteorite and Their Mode of Formation, Geochim. Cosmochim. Acta 29, 773-779 (1965).

Moore, C. B., Birrell, P. J. and Lewis, C. F., Variations in the Chemical and Mineralogical Composition of Rim and Plains Specimens of the Canyon Diablo Meteorite, Geochim. Cosmochim. Acta 31, 1885-1892 (1967).

Moore, C. B., Lewis, C. F. and Nava, D., Superior Analyses of Iron Meteorites, in "Meteorite Research", (ed. P. M. Millman), Springer-Verlag, New York, 738-748 (1969).

Nininger, H. H., Structure and Composition of Canyon Diablo Meteorites as Related to Zonal Distribution of Fragments, Popular Astron. 58, 169-173 (1950).

Nininger, H. H., Out of the Sky, An Introduction to Meteoritics, Dover Publications Inc., New York (1952).

Nininger, H. H., Arizona's Meteorite Crater, American Meteorite Museum, Sedona, Arizona, p. 81-114 (1956).

Olshaker, A. E. and Bjork, R. L., Hydrodynamics Applied to Hypervelocity Impact. II. The Role of Melting and Vaporization in Hypervelocity Impact, Proc. Symp. Hypervelocity Impact, 5th, Colorado School of Mines, Colorado, 1, Part 1, 225-239 (1961).

Öpik, E. J., Meteorite Impact on Solid Surface, Irish Astron. J., 5, 14-33 (1958).

Petrowski, C., Kerridge, J. F. and Kaplan, I. R., Light Element Geochemistry of the Apollo 17 Site, Proc. Fifth Lunar Sci. Conf., Suppl. 5, Vol. 2, Geochim. Cosmochim. Acta, 1939-1948 (1974).

Ramdohr, P., Iron-Spherulites in the Vicinity of the Canyon Diablo Crater and a Comparison with the Cosmic Spherulites of the Deep Sea Sediments, Chem. Erde 25, 259-281 (1966)(in German).

Rees, C. E., A Steady-State Model for Sulphur Isotope Fractionation in Bacterial Reduction Processes, Geochim. Cosmochim. Acta 37, 1141-1162 (1973).

Rees, C. E. and Thode, H. G., Sulfur Concentrations and Isotope Ratios in Apollo 16 and 17 Samples, Proc. Fifth Lunar Sci. Conf., Geochim. Cosmochim. Acta, Vol. 2, 1963-1973 (1974).

Rinehart, J. S., Distribution of Meteoritic Debris About the Arizona Meteorite Crater, Smithson. Contrib. Astrophys. 2, 145-160 (1958).

Rostoker, N., The Formation of Craters by Highspeed Particles, Meteoritics 1, 11-27 (1953).

Sakai, H. and Yamamoto, M., Fractionation of Sulphur Isotopes in the Preparation of Sulphur Dioxide. An Improved Technique for the Precision Analysis of Stable Sulphur Isotopes, Geochemical Journal 1, 35-42 (1966).

Spencer, L. J., Meteoric Iron and Silica-Glass from the Meteorite Craters of Henbury (Central Australia) and Wabar (Arabia), Mineral. Mag. 23, 387-404 (1933).

Thode, H. G., Sulphur Isotope Geochemistry, Studies in Analytical Geochemistry, The Royal Society of Canada, Special Publications No. 6, (Shaw, D. M., ed.), University of Toronto Press, 25-41 (1963).

Thode, H. G., Sulphur Isotope Geochemistry and Fractionation Between Coexisting Sulphide Minerals, Mineral. Soc. Amer. Spec. Pap. 3, 133-144 (1970).

Thode, H. G., Monster, J. and Dunford, H. B., Sulphur Isotope Geochemistry, Geochim. Cosmochim. Acta 25, 150-174 (1961).

Thode, H. G. and Rees, C. E., Measurement of Sulphur Concentrations and the Isotope Ratios $^{33}S/^{32}S$, $^{34}S/^{32}S$ and $^{36}S/^{32}S$ in Apollo 12 Samples, Earth Planet. Sci. Lett. 12, 434-438 (1971).

Thode, H. G. and Rees, C. E., Sulphur Isotopes in Grain Size Fractions of Lunar Soils, Proc. Seventh Lunar Sci. Conf., Suppl. 7, Vol. 2, Geochim. Cosmochim. Acta (1976) (in press).

Vand, V., Astrogeology: Terrestrial Meteoritic Craters and the Origin of Tektites, Advan. Geophys. 11, 1-114 (1965).

Wanless, R. K. and Thode, H. G., A Mass Spectrometer for High Precision Isotope Ratio Determinations, J. Sci. Instr. 30, p. 395 (1953).

Weast, R. C., (ed.), Handbook of Chemistry and Physics, 49th Edition, published by the Chemical Rubber Co., Cleveland, Ohio, p. B-208 (1968).